Article

Immunity

Distinct Effector B Cells Induced by Unregulated Toll-like Receptor 7 Contribute to Pathogenic Responses in Systemic Lupus Erythematosus

Graphical Abstract

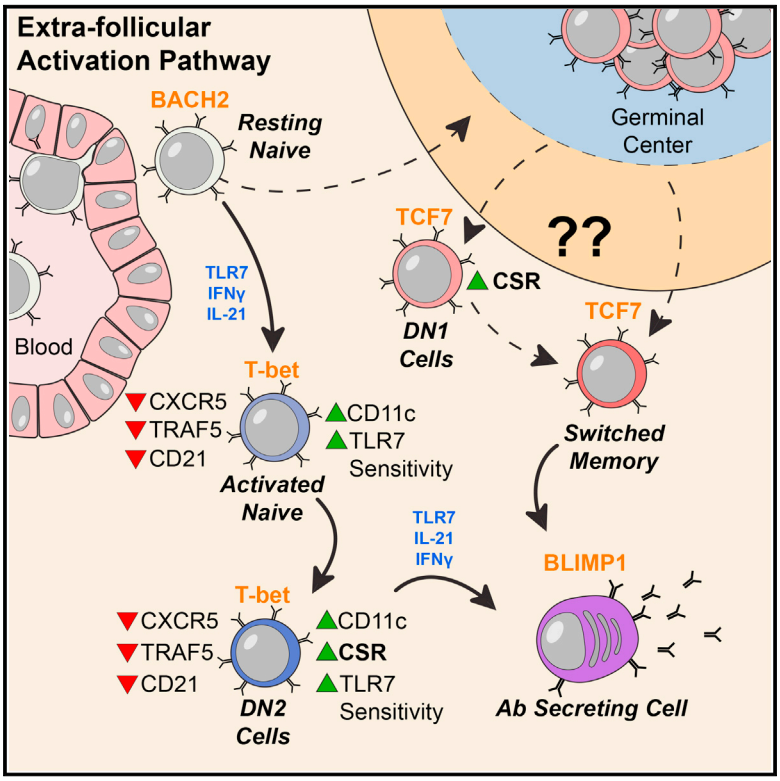

Highlights

- Autoreactive CD27^{-} IgD^{-} CXCR5^{-} CD11c^{+} (DN2) B cells expand in lupus patients
- DN2 cells derive from naive cells and are poised to generate plasmablasts
- DN2 B cells are hyper-responsive to Toll-like receptor-7 signaling
- The properties of SLE DN2 B cells stem from distinct transcriptional networks

Authors

Scott A. Jenks, Kevin S. Cashman, Esther Zumaquero, ..., Jeremy M. Boss, Frances E. Lund, Ignacio Sanz

Correspondence

ignacio.sanz@emory.edu

In Brief

The role of extrafollicular B cells in human systemic lupus is unknown. Jenks et al. define the main components of this pathway and its prominence in severe disease. Its activation is mediated by hyper-responsiveness to Toll-like receptor-7 and leads to the generation of autoreactive antibody-secreting plasmablasts.

Jenks et al., 2018, Immunity *49*, 1–15
October 16, 2018
https://doi.org/10.1016/j.immuni.2018.08.015

CellPress

Please cite this article in press as: Jenks et al., Distinct Effector B Cells Induced by Unregulated Toll-like Receptor 7 Contribute to Pathogenic Responses in Systemic Lupus Erythematosus, Immunity (2018), https://doi.org/10.1016/j.immuni.2018.08.015

Distinct Effector B Cells Induced by Unregulated Toll-like Receptor 7 Contribute to Pathogenic Responses in Systemic Lupus Erythematosus

Scott A. Jenks,[1,9] Kevin S. Cashman,[1,9] Esther Zumaquero,[2,9] Urko M. Marigorta,[3] Aakash V. Patel,[1] Xiaoqian Wang,[1] Deepak Tomar,[1] Matthew C. Woodruff,[1] Zoe Simon,[1] Regina Bugrovsky,[1] Emily L. Blalock,[1] Christopher D. Scharer,[8] Christopher M. Tipton,[1] Chungwen Wei,[1] S. Sam Lim,[1] Michelle Petri,[4] Timothy B. Niewold,[5] Jennifer H. Anolik,[6] Greg Gibson,[3] F. Eun-Hyung Lee,[7] Jeremy M. Boss,[8] Frances E. Lund,[2] and Ignacio Sanz[1,10,*]

[1]Department of Medicine, Division of Rheumatology, Lowance Center for Human Immunology, Emory University, Atlanta, GA, USA
[2]Department of Microbiology, The University of Alabama at Birmingham, Birmingham, AL, USA
[3]Center for Integrative Genomics, Georgia Institute of Technology, Atlanta, GA, USA
[4]Hopkins Lupus Center, Department of Medicine, Johns Hopkins University, Baltimore, MD, USA
[5]Colton Center for Autoimmunity, NYU School of Medicine, New York, NY, USA
[6]Division of Allergy, Immunology and Rheumatology, University of Rochester Medical Center, Rochester, NY, USA
[7]Division of Pulmonary, Allergy and Critical Care, Emory University, Atlanta, GA, USA
[8]Department of Microbiology and Immunology, Emory University, Atlanta, GA, USA
[9]These authors contributed equally to this work
[10]Lead contact
*Correspondence: ignacio.sanz@emory.edu
https://doi.org/10.1016/j.immuni.2018.08.015

SUMMARY

Systemic Lupus Erythematosus (SLE) is characterized by B cells lacking IgD and CD27 (double negative; DN). We show that DN cell expansions reflected a subset of CXCR5$^-$ CD11c$^+$ cells (DN2) representing pre-plasma cells (PC). DN2 cells predominated in African-American patients with active disease and nephritis, anti-Smith and anti-RNA autoantibodies. They expressed a T-bet transcriptional network; increased Toll-like receptor-7 (TLR7); lacked the negative TLR regulator TRAF5; and were hyper-responsive to TLR7. DN2 cells shared with activated naive cells (aNAV), phenotypic and functional features, and similar transcriptomes. Their PC differentiation and autoantibody production was driven by TLR7 in an interleukin-21 (IL-21)-mediated fashion. An *in vivo* developmental link between aNAV, DN2 cells, and PC was demonstrated by clonal sharing. This study defines a distinct differentiation fate of autoreactive naive B cells into PC precursors with hyper-responsiveness to innate stimuli, as well as establishes prominence of extra-follicular B cell activation in SLE, and identifies therapeutic targets.

INTRODUCTION

Systemic lupus erythematosus (SLE) is an autoimmune disease with multiple associated autoantibodies. Accordingly, circulating antibody secreting cells (ASC) are prominent in flaring SLE. We reported that a large fraction of these ASC originate from activated naive B cells (aNAV), of distinct phenotype (Tipton et al., 2015). We also described the expansion of class-switched B cells lacking IgD and the B cell memory marker CD27 (double negative; DN) (Wei et al., 2007). Similar DN cells have been described as exhausted atypical memory cells in HIV and malaria patients and as anergic naive B cells (Isnardi et al., 2010; Moir et al., 2008). However, the significance of DN cells remains unclear. Thus, we performed a comprehensive interrogation of these cells in SLE. Our results indicate that the expansion of DN cells in SLE are accounted for by a CXCR5$^-$ CD21$^-$ CD11c$^+$ subset (DN2) lacking FCRL4, a marker of atypical memory cells (Ehrhardt et al., 2008) that mediates hypo-responsiveness in HIV infection. DN2 cell expansion was most prominent in African-American patients with high disease activity and nephritis and strongly correlated with anti-Smith and anti-RNA autoantibodies. DN2 cells and aNAV cells shared markers that separated them from other B cells and have a highly similar transcriptomes with high amounts of T-bet and Zeb2. Poised PC differentiation was indicated by phenotypic, functional, transcriptional, and epigenetic data, as well as clonal sharing with circulating plasmablasts (PB). Finally, DN2 cells expressed low amounts of negative TLR regulators including TRAF5. Accordingly, they displayed enhanced responsiveness to TLR7 stimulation. Our work defines a distinct extra-follicular B cell differentiation pathway responsible for the expansion of effector B cells in active SLE. Understanding the antigenic triggers and molecular landscape of DN2 cells should provide pathogenic insight and identify therapeutic targets.

RESULTS

A Subset of IgD$^-$ CD27$^-$ B Cells Lacking CXCR5 Is Highly Expanded in SLE

DN B cells were studied by flow cytometry in two SLE cohorts. SLE-1 (N = 40; University of Rochester and Johns Hopkins

University), included patients with lower disease activity. SLE-2 (N = 50; Emory University), was enriched for higher disease activity and higher serum autoantibodies. After excluding $CD38^{hi}$ $CD27^{hi}$ PB, $CD19^+$ B cells were classified into four populations: switched memory (SWM, IgD^-CD27^+); unswitched memory (USW, IgD^+ $CD27^+$); naive (NAV, IgD^+CD27^-); and IgD^- $CD27^-$ (DN cells). As in previous studies B cell homeostasis was abnormal in both cohorts (Figures 1A–1D), with SLE patients showing marked decreases of USW cells and large increases of DN cells. Two DN cell subsets (DN1 and DN2) were defined by CXCR5, CD19, and CD21 (Figures 1B and 1C). DN1 cells, expressing the B cell follicle homing receptor CXCR5 and intermediate amounts of CD19, represented the majority of DN cells in HCD. In contrast, DN2 cells defined by the absence of CXCR5 and CD21 and high CD19, represented the majority of DN cells expanded in SLE (Figures 1B and 1C). DN2 cells were characterized by high surface expression of the alpha integrin CD11c, primarily expressed in dendritic cells and monocytes, but also found in extra-follicular PB (Racine et al., 2008) and age-associated B cells (ABCs) (Rubtsova et al., 2015) (Figure 1D). While DN2 cells were a minor component of $CD19^+$ and DN B cells in HCD, they represented a much higher fraction in SLE where they may account for the majority of non-plasmablast $CD19^+$ B cells (Figures 1E and 1F). Absolute numbers of DN2 cells were also greatly increased in SLE patients with high DN2 frequency (Figure 1G). While DN2 cell frequencies were elevated in some patients with rheumatoid arthritis (RA) and systemic sclerosis, the highest frequency occurred in SLE and was not elevated in primary Sjögren's syndrome patients (Figure 1F).

DN2 Cells Share a Distinct Phenotype with Activated Naive B Cells

DN2 cells were characterized by the absence or low expression of CD24 and CD38 proteins expressed by most human peripheral B cells (Figures 2A and 2B). DN2 also expressed low amounts of lymph node homing receptor L-selectin (CD62L) and had higher expression of regulatory receptors CD32b and (Siglec-2) CD22. Other proteins with higher expression in DN2 included activation markers CD69, HLA-DR, and CD86.

We recently defined a population of activated naive B cells (aNAV), also characterized by high CD19 and loss of CD21, which is expanded in SLE and represents a major source of antibody secreting plasma cells (PC) (Tipton et al., 2015). aNAV represented the only B cell population sharing multiple DN2 markers, including lack of CXCR5, CD24, and CD38, high expression of CD11c and retention of Mitotracker green (Figures 1D and 2B and 2C).

Murine $CD11c^{bright}$ ABCs are important for the development of anti-viral IgG2a and autoimmune responses (Rubtsova et al., 2015). IgG3, the human IgG2a equivalent represents the dominant IgG subclass deposited in lupus kidneys (Zuniga et al., 2003). DN2 cells expressed mostly sIgG with a higher frequency of $IgG3^+$ cells than SWM or DN1 cells in both HCD and SLE patients (Figure 2D). Of note, DN2 cells displayed 50% lower amounts of sIgG (Figure 2E).

DN2 cells resemble IgD^-, $CD27^-$, CD21-, $CD11c^+$ extra-follicular tonsil B cells (Ehrhardt et al., 2008) and similar cells found in RA synovial fluid (Yeo et al., 2015) and in the blood of HIV patients, with the latter representing exhausted memory cells (Moir et al., 2008). Both tissue-based and exhausted memory B cells are defined by the inhibitory Fc receptor homolog, FCRL4, that impairs exhausted memory B cells (Kardava et al., 2011). As expected, FCRL4 was expressed in HIV $CD21^-$ DN but not in SLE DN2 cells (Figure 2E). However, FCRL5, which is induced by BCR signaling and can drive naive B cell proliferation (Davis et al., 2001; Dement-Brown et al., 2012), is expressed in SLE DN2 and aNAV B cells. A similar FcRL4/5 pattern has been reported in malaria patients for $CD21^-$ atypical memory cells with impaired proximal B cell signaling (Portugal et al., 2015). However, as shown in Figure 2G, BCR cross-linking induces substantial BLNK phosphorylation in SLE DN2 cells despite expressing less surface IgG and higher amounts of FCRL5, CD32b, and CD22.

SLE Patients with Increased DN2 B Cells Are Predominantly African American with Active Disease and anti-smith/RNP and RNA Autoantibodies

The highest frequency of DN2 cells was found in the SLE-2 cohort with a predominance of African-American patients (AA) (Figure 1A). As shown in Figure 3A, AA patients have a significantly higher frequency of DN2 even in a cohort-independent fashion as it is also observed in SLE-1 despite a predominance of European-American patients. A higher frequency of DN2 cells was present in AA patients with low-medium disease activity relative to non-AA patients ($p = 0.0376$). In RA patients, the frequency of DN2-like $CD11c^+$ ABC B cells increases with age in women (Rubtsov et al., 2011). We found no age relationship in SLE (Figure 3B), where large expansions of DN2 cells were present in young children (Figure 3C). The frequency of DN2 cells had modest yet significant correlation with disease activity (Figure 3D), to a degree commensurate with other immunological variables including plasmablast frequency (Jacobi et al., 2003). Overall disease activity was higher in patients with expanded DN2 cells and a strong association was present in nephritis patients (Figure 3D). Consistent with more active disease, a larger fraction of high DN2 patients were treated with glucocorticoids (Figure 3E). DN2 cell frequency was modestly correlated with serum type I interferon activity in both cohorts despite the higher frequency in SLE-2 of AA patients, a population with higher type I IFN activity (Weckerle et al., 2010) (Figure 3F). Serologically, high DN2 patients had higher titers of anti-RNA antibodies and were much more likely to have anti-Sm reactivity (Figures 3G and 3H). Moreover, using a highly quantitative luciferase immunoprecipitation assay (LIPS) (Ching et al., 2012), a strong positive correlation was observed with contemporaneous anti-Sm and anti-RNP titers but not other autoantibodies (Figure 3I).

VH4-34-encoded ($9G4^+$) autoantibodies are highly specific for SLE and contribute substantially to dsDNA, Smith and Ro autoantibodies, as well as to anti-lymphocyte and apoptotic cell binding (Richardson et al., 2013; Tipton et al., 2015). The frequency of $9G4^+$ cells is increased among aNAV cells in flaring SLE (Tipton et al., 2015) and in global DN cells (Wei et al., 2007). Consistently, we found in the current study, an increased frequency of $9G4^+$ B cells in DN2 cells relative to SWM cells and in aNAV relative to resting naive (Figures S1A and S1B). Patients with expanded DN2 cells were also enriched for serum $9G4^+$ anti-B cell autoantibodies (Richardson et al., 2013) (Figure S1C).

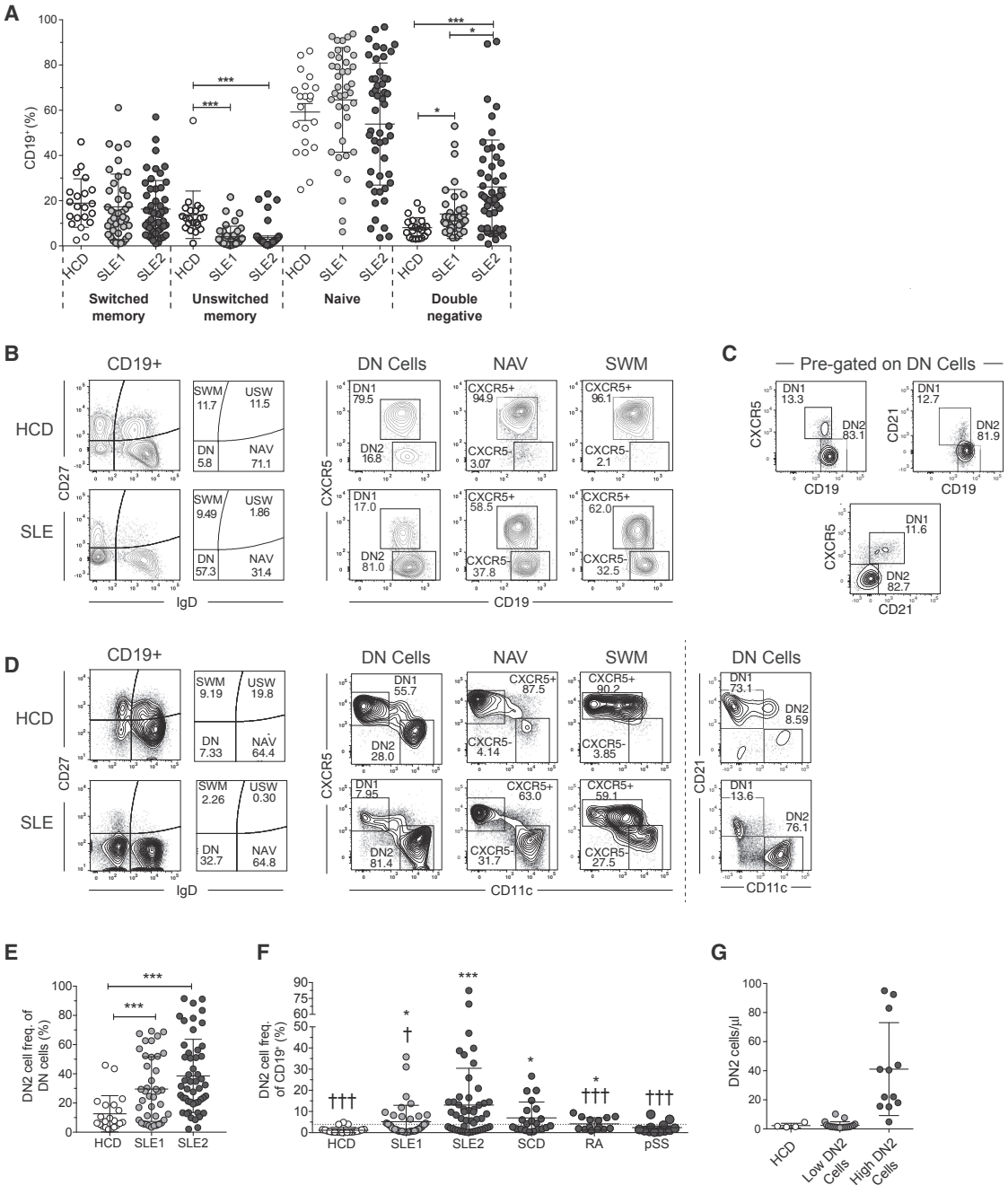

Figure 1. IgD- CD27- DN B Cells in SLE

(A) B cell populations in SLE and HCD. Parental $CD19^+$ populations defined by IgD and CD27: IgD-$CD27^+$ (switched memory; SWM); IgD^+CD27^+ (unswitched memory; USW); IgD^+ $CD27^-$ (naive; NAV); IgD-$CD27^-$ (double negative; DN cells). Mean ± SD shown for HCD n = 21, SLE1 n = 40, SLE2 n = 50, Welch's t test.

(B) In HCD most DN B cells are $CXCR5^+$ (DN1 cells) with a minor fraction (DN2 cells) lacking CXCR5 and expressing high amounts of CD19. Representative examples of large DN2 cells expansions in SLE (n = 8), where they become the largest DN fraction.

(C) $CXCR5^-$, CD19 ^{bright} DN2 cells are $CD21^-$.

(D) DN2 cells are CD11c ^{bright}.

(E) A higher proportion of DN cells are DN2 cells in SLE patients than HCD (Welch's t test).

(F) The frequency of DN2 cells in SLE cohorts, rheumatoid arthritis (RA, n = 15), primary Sjögren's syndrome (pSS, n = 11), and scleroderma patients (SCD, n = 21). Dotted line indicates the mean of the HCD frequency plus 2 SD (4.01%).

(G) Absolute number of DN2 cells/µl in SLE patients from cohort 2 with (n = 11) or without (n = 21) DN2 cell expansion.

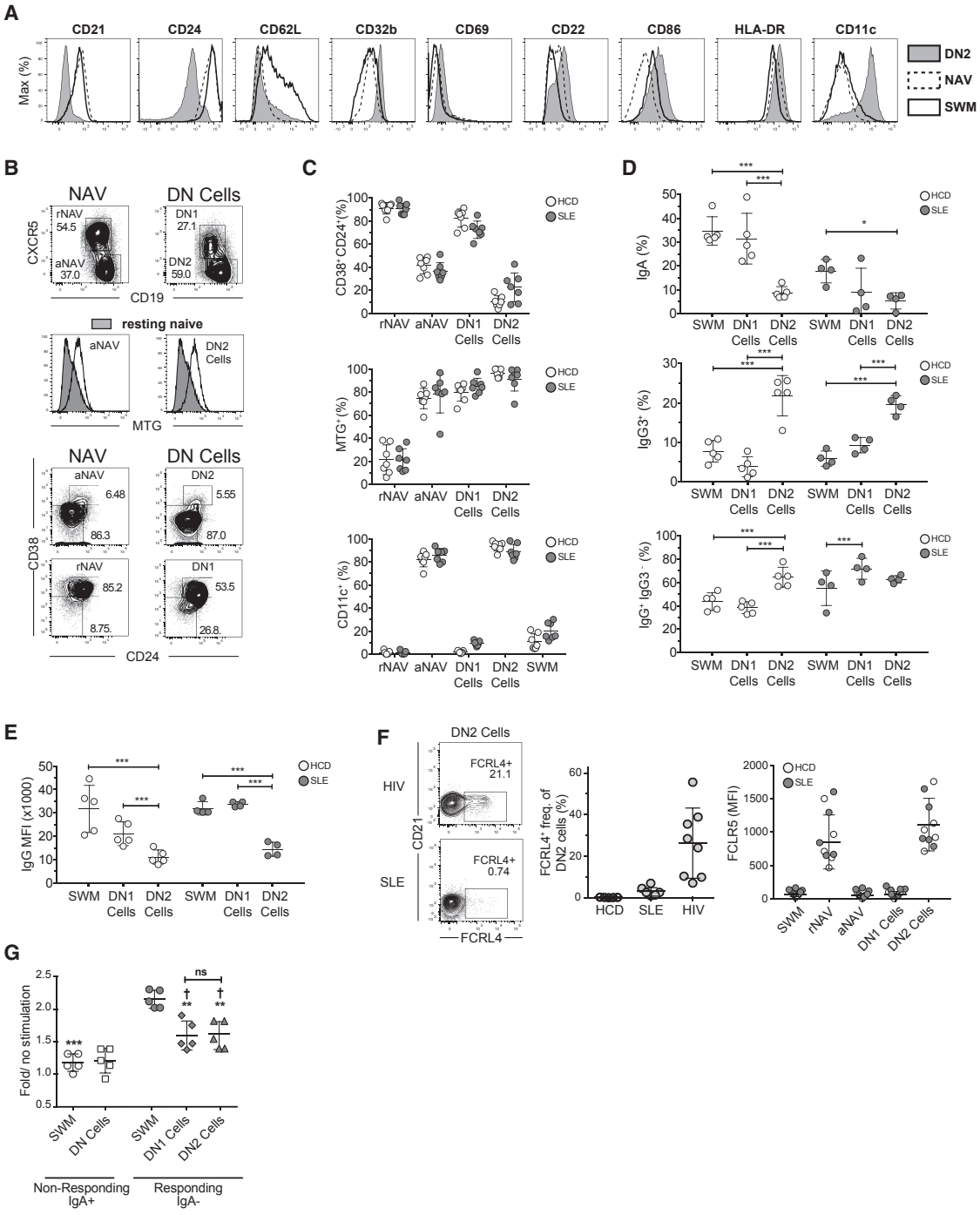

Figure 2. Phenotype of SLE DN2 B Cells

(A) Surface staining of SLE B cells for the indicated markers. DN2 cells (shaded) are compared to NAV (dotted line) and SWM (solid line) B cells.

(B) Representative (n = 8) flow cytometry from active SLE. NAV and DN cells are separated based on CXCR5 and CD19 into DN1 cells, DN2 cells, rNAV (IgD^+, $CXCR5^+$, $CD19^+$), and aNAV (IgD^+, $CXCR5^-$, $CD19^{bright}$). MTG is positive for both DN2 cells and aNAV (open) but negative for rNAV (filled).

(C) aNAV and DN2 cells are $CD24^-$ $CD38^-$, MTG^+, and $CD11c^{bright}$ SLE and HCD.

(D) Frequency of IgA^+, $IgG3^+$, and non-IgG3 IgG^+ for the indicated subsets in HCD (n = 5) and SLE (n = 4) patients (Mean ± SD) (Welch's t test).

(E) IgG^+ DN2 cells have lower surface IgG than DN1 cells or SWM in both HCD and SLE (Mean ± SD).

(legend continued on next page)

SLE B Cells Have Higher Expression of Interferon Regulated Genes and Nucleic Acid Sensors and Lower Expression of Negative Regulators

RNA sequencing was used to analyze the transcriptome DN1 cells, DN2 cells, SWM, and total NAV B cells. A total of 154 differentially expressed genes (DEG) segregated SLE from HCD B cells. Three distinct cell clusters were defined in HCD and two SLE patients: NAV, SWM-DN1 cells, and DN2 cells. In the third patient (SLE3), all four B cell subsets clustered closer together owing to higher transcription of DEG expressed in SLE B cells. SLE3 had active nephritis and a high fraction of aNAV cells (30% of all naive cells; data not shown).

Principal component 1 (PC1) separated HCD from SLE for all subsets and had higher values for NAV cells in SLE3 (Figure S2B). PC1 genes highly expressed in SLE included the transcription factors (TF) STAT1 and STAT2 and other interferon regulated genes (Figure S2C). The participation of this pathway was supported by the identification by gene set enrichment analysis (GSEA; Figure S2D) of the overexpression of all three interferon-induced modules defined in SLE mononuclear cells, including IFN-β and IFN-γ (Chiche et al., 2014).

Notably, the SLE B cell transcriptome was enriched for sensors of viral RNA, including TLR7 and *IFIH1* (Figures S2C and S2D). Also increased were dsDNA sensors, including inducers of inflammatory pathways of pathogenic relevance for SLE such as the STING inducer *TRIM56*. SLE B cells also overexpressed the *TBK1* kinase that is activated downstream of TLR7 and cytosolic DNA and dsRNA sensors (Kawai and Akira, 2010).

A minority of DEG were downregulated in SLE B cells including TNF-induced genes such as the negative signaling regulators *NFKBIA* and *TNFAIP3*, the latter representing a major SLE susceptibility gene (Musone et al., 2008) (Figures S2C and S2D).

DN2 B Cells Are Characterized by a Unique Pattern of Transcription Factors, Cytokine Receptors, and Negative Regulators of Signaling

Comparative analysis identified 2,154 genes DEGs between any of the four B cell subsets and demonstrated a distinct DN2 transcriptome. As shown in Figures 4A and S3A, DN2 and NAV cells clustered independently from each other and from DN1 and SWM which in turn, displayed almost identical transcriptomes with only 22 DEGs (Figures 4A and 4B). In contrast, over 1,000 DEGs separated DN2 from NAV and SWM cells. PC1 separated DN2 cells from other B cells and PC2 separated NAV B cells from SWM, DN1, and DN2 cells. Reflecting a high content in aNAV cells, NAV B cells from SLE3 had a higher PC1 value and were closer to DN2. This hypothesis was experimentally tested by RNA-seq of the corresponding fractions from additional SLE patients, which demonstrated highly similar transcriptomes of aNAV and DN2 cells (Figures S4A and S4B).

Validating the RNA-seq data, there was complete concordance between transcriptional and protein expression of multiple key genes identified by flow cytometry including CD11c, CD86, FCGR2B, FCRL5, and FCRL4.

B cell subpopulations did not differ in their expression of type I IFN receptors and had equal responses to IFN-α (Figures S5A–S5F). Instead, DN2 cells expressed higher type III IFN-λ receptor *IFNLR1*, *IL10RA*, and *IL10RB* (Figure 4C). Expression of IL-10Rα was verified by flow cytometry (Figure S5C) and expression of IL-10R and IFN-λR were confirmed functionally (Figures S5D–S5F). Heightened response to IFN-λ and IL-10 was only shared by aNAV cells.

Several informative TF were preferentially expressed in DN2 cells prominently including *TBX21* (T-bet) and the T-bet-induced transcriptional regulator *ZEB2* (Figure 4D and Figure S4C). Flow cytometry confirmed T-bet overexpression in DN2 and aNAV (Figure 4D). Moreover, DN2 cells expressed higher amounts of IRF4, a TF essential for PC differentiation (Xu et al., 2015). An IRF4-induced transcriptome in DN2 cells was also documented by higher expression of genes with binding motifs for IRF4 and its co-factor SPI1 (PU.1) (Figure 4F).

The transcriptional identity of DN2 cells was also determined by low transcription of immunologically relevant genes including the sorting marker CXCR5 and other surface markers assessed by flow cytometry including CD24 and CR2. Also, uniquely low in DN2 cells were regulators of TNF receptor-associated factor (TRAF) protein interactions *TRAF5*, *TNFAIP3*, and *TRAF3IP2*. DN2 cells also had low expression of anti-apoptotic *BCL2* and *ZEB1*, a transcriptional regulator whose binding motifs were enriched in genes with low DN2 expression including *CXCR5*, *CD21*, and *TRAF5* (Figures 4E and 4F).

PC2 separated NAV from SWM cells while showing similarity between SWM and DN1 cells. The positive scores for DN2 cells were driven by overexpression of genes including the BLIMP1 repressor *BCL6*, the inhibitory protein *CD72*, and the cytokine receptor *IL21R* (Figure 4C). *IL21R*, critical for naive B cell differentiation, was higher in DN2 cells than in SWM and had the highest expression in NAV and aNAV cells (Figure S4C). These differences were confirmed functionally through IL-21-induced STAT3 phosphorylation (Figure S5B). However, DN2 cells lacked expression of some genes highly transcribed in NAV cells, namely transcriptional repressors and negative regulators of effector B cell differentiation, including *BACH2*, *FOXP1*, *BCOR*, *SPRY*, and *FOXO1* (Kometani et al., 2013; Rao et al., 2012). Further reflecting their relatedness with DN2 cells, this pattern was shared by aNAV cells (Figure S4C). Genes with higher expression in SWM relative to DN2 cells and NAV B cells included the high-affinity IL-2 alpha receptor (*IL2RA*; CD25), and the central T cell memory transcription factors *TCF7* and *RORA* (Figures 4C and 4E).

GSEA analysis (Figure S3B) showed that genes enriched in DN2 cells had higher expression in published transcriptomes of NAV B cells, total lupus B cells, and PC. The DN2 B cell transcriptome was also enriched in gene sets from effector memory

(F) Unlike HIV CD21- DN cells, SLE DN2 cells do not express FCRL4. On the left, representative (n = 5) flow profiles comparing CD21 and FCRL4 for HIV and SLE DN cells, followed by the percent of $CD21^-$ DN cells that are $FCRL4^+$ for HCD (5), HIV (8), and SLE (6) patients. On the right, the mean fluorescence intensity of FCRL5 staining is shown for different B cell populations from SLE patients (filled; n = 5) and HCD (open; n = 5) (Mean ± SD, n = 7).

(G) Proximal BCR signaling is intact in DN2 cells as indicated by BLNK phosphorylation fold increase after anti-IgG stimulation. Values are shown for non-responding (IgA^+) or responding (IgA^-) cells (n = 5; * = p value relative to responding SWM; † = p value relative to non-responding total DN, repeated-measure one-way ANOVA).

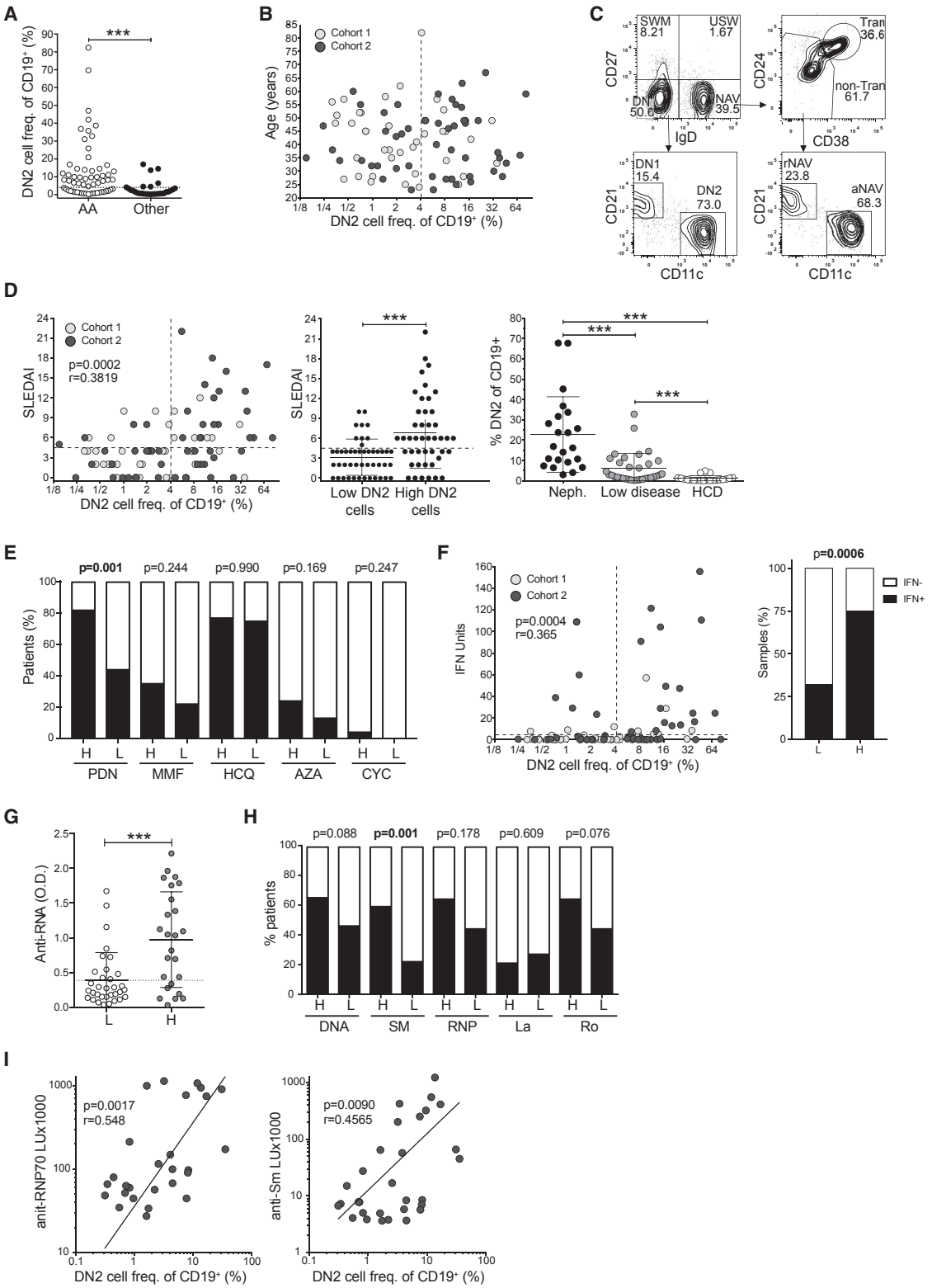

Figure 3. Clinical and Demographic Correlates of Patients with Expanded DN2 Cells

(A) African American (AA) patients (n = 61, open symbol) have significantly higher proportions of DN2 cells relative to non-AA patients (n = 29, closed symbol) (Mean ± SD, Welch's t test).

(B) Lack of correlation between the DN2 cell frequency of $CD19^+$ B cells and age in SLE cohorts. The percentage of DN2 is shown on a $\log_2$ scale.

(C) Flow profile of a 5-year-old female lupus patient in whom most $CD19^+$ cells are DN2 cells and aNAV.

(legend continued on next page)

T cells, whereas SWM cells shared their transcriptional profile with central memory T cells. The similarity between DN2 cell transcriptomes and unfractionated SLE B cells suggests a predominance of this cell subset among total lupus B cells in previous studies.

Transcriptional and Functional Analysis Identify SLE DN2 Cells as Precursors of Autoantibody Producing Plasma Cells

Consistent with the enrichment for IRF4-binding motifs, GSEA indicated that, relative to SWM, DN2 cells transcribed higher amounts of IRF4 target genes expressed by PC (Figure 5A). This pattern is illustrated by SLAMF7, a lymphocyte activation molecule highly expressed by PC, which is also upregulated by DN2 and aNAV cells but no other B cells (Figure 5B).

IRF4 and IRF8 reciprocally regulate each other to determine PC versus germinal center fates (Xu et al., 2015). *IRF4* transcription was higher in SLE DN2 cells than in SWM whereas *IRF8* expression was lower than in other B cell populations (Figure 5C). Also indicative of a PC differentiation fate, DN2 cells expressed low amounts of *ETS1* (Figure 5C), a TF that represses PC differentiation (Luo et al., 2014). Finally, expression of *PRDM1* (BLIMP-1), an IRF4-induced transcriptional repressor that silences B cell programs and induces PC differentiation (Nutt et al., 2015), was upregulated in DN2 relative to rNAV cells (Figure 5C). In keeping with this pattern, ATAC-seq demonstrated opening of the *PRDM1* locus in aNAV and DN2 cells (Figure S6), and flow cytometry demonstrated higher protein expression of BLIMP-1 in aNAV and DN2 cells relative to any other cell types other than PC (Figure 5D). Flow cytometry also confirmed that DN2 cells and aNAV cells express significantly higher amounts of IRF4 than rNAV and DN1 cells and that the IRF8/IRF4 ratio is significantly lower in aNAV and DN2 cells. This profile is consistent with the promotion of a PC rather than memory fate (Figure 5E).

In keeping with a PC differentiation fate, DN2 cell expansions were common in patients with high PC frequencies (Figure S7A). Yet, in other conditions, DN2-like cells appeared to poorly differentiate into ASC, typically after BCR and TLR9 stimulation in the absence of exogenous cytokines (Moir et al., 2008; Portugal et al., 2015). In contrast, we found that DN2 cells were highly responsive to inducers of ASC differentiation including TLR7, IL-21, and IL-10. Indeed, despite lacking significant increase in numbers by day 7, DN2 cells produced higher amounts of IgG on a per cell basis relative to DN1 cells and SWM (Figure 5F). Consistently, ELISPOT readouts identified IgG ASC frequencies higher than rNAV and comparable to SWM and DN1 cells (Figure 5G). Of note, DN2 cells but not SWM or DN1 cell differentiation was dependent on IL-21 and IL-2 (Figure 5H). LIPS measurement of culture supernatants showed that DN2 cells produced anti-Smith, anti-RNP, or anti-Ro antibodies in a pattern consistent with the serological profile of the corresponding patient and in amounts comparable to SWM cells (Figure 6I).

BCR sequencing showed that the IgG mutation rate was similar in DN2 cells and PC but lower than SWM (Figure S7B). These results strongly argue against direct DN2 differentiation from memory cells or through additional cycles of germinal center maturation of pre-existing memory cells as both paths should result in stable or increased frequency of mutation in DN2 cells, respectively (Figure S7B). Bulk sequencing and high throughput single-cell sequencing demonstrated a substantial degree of clonal connectivity between DN2 cells and PC, thereby providing *in vivo* evidence of PC differentiation from DN2 cells (Figures S7D and S7E). Similarly, BCR sequencing of aNAV, DN2 cells, and PC showed expanded clones shared between all three populations (Figure S7F).

Combined, our studies provide transcriptional, epigenetic, and functional *in vitro* evidence for the potential of DN2 cells to differentiate into PC, which was in turn corroborated *in vivo* by extensive BCR repertoire clonal sharing.

DN2 Are Hyper-Responsive to TLR7 but Not CD40 Stimulation

DN2 and aNAV cells expressed the lowest amount of *TRAF5* (Figure 4E, Figure S4C), an essential mediator of CD40 signaling and the main negative regulator of TLR signaling in mouse B cells (Buchta and Bishop, 2014). Accordingly, CD40L stimulation increased CD25 expression in NAV, but not in DN2 cells (Figure 6A). In contrast, TLR7 stimulation strongly induced CD25 and ERK and MAPKp38 phosphorylation in DN2 cells but not in other B cells (Figures 6B and 6C). TLR7 hyper-responsiveness was shared by aNAV cells (Figures 6C and 6D). In keeping with enhanced TLR7 responsiveness, R848-stimulated DN2 cells upregulated expression of HLA-DR and CD86 relative to SWM and NAV B cells (Figure 6E). In contrast, two negative regulators of B cell receptor signaling, CD72 and CD32b, were downregulated by TLR7 stimulation in DN2 cells, but not NAV B cells. DN2 cells from HCD responded similarly except for CD72 whose expression was unaltered.

(D) Positive correlation between DN2 cell frequency and high disease activity using Spearman's r coefficient (left panel). Median SLEDAI is plotted against the percentage of DN2 cells with the dotted line indicating the cut-off for expanded DN2 cells (left panel). Middle panel: SLEDAI in patients with or without DN2 cell expansion. Right panel: frequency of DN2 cells in patients with active lupus nephritis (n = 22), patients with low disease activity (n = 33) and HCD (n = 21).

(E) Patients with expanded DN2 cells are more likely to be treated with prednisone (PDN). The percentage of patients treated is shown in black and untreated in white for patients with high (H) or low (L) DN2 cell frequencies. P value is shown for Fischer's exact test. Mycophenolate mofetil (MMF); hydroxychloroquine (HCQ); azathioprine (AZA); cyclophosphamide (CYC).

(F) Correlation between serum interferon activity and percent of DN2 cells (Spearman's r coefficient). Right panel: Patients with higher DN2 frequencies were more likely to have increased serum IFN activity.

(G) Serum anti-RNA antibody concentrations in patients with low (L, n = 33) or high (H, n = 25) frequencies of DN2 cells. The dotted line is the mean OD for HCD serum (Mean ± SD, Welch's t test).

(H) The percentage of samples that are positive (black) for each of the indicated serologies in patients with a high (H) and low (L) frequency of DN2 cells (Fischer's exact test);

(I) Anti-Smith-D and anti-RNP-70 serum antibody titers from patients from cohort 1 measured by LIPS assay correlate with the percentage of DN2 cells (Spearman's r coefficient).

Please also see Figure S1.

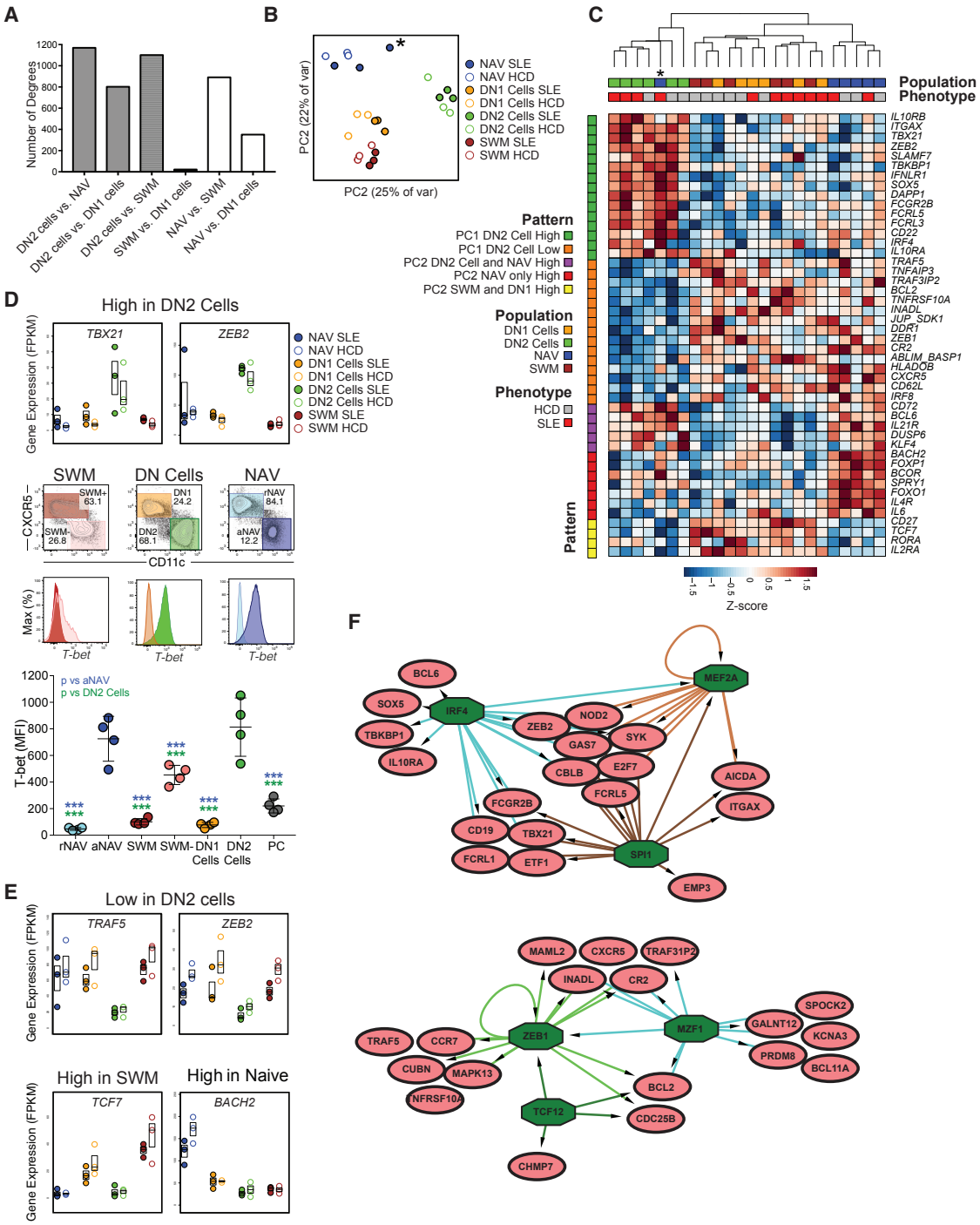

Figure 4. DN2 Cells Gene Expression Is Distinct from Other B Cell Populations

(A) Number of differentially expressed genes (DEG), between each B cell subset of pooled HCD and SLE samples.

(B) Analysis of principal components accounting for 47% of the variance between B cell subsets. Patients groups and cell subsets are indicated. * identifies NAV B cells from the lupus nephritis patient (SLE3), with a large fraction of aNAV cells.

(C) Heatmap of select DEG that differentiate B cell subsets. Samples are clustered based in Euclidian distance. In SLE-3 (*), NAV cells cluster with the DN2 cells. Genes are grouped by expression pattern as shown in the legend.

(D) DN2 cells highly express *TBX21* and *ZEB2*. The top panel represents FPKM (Fragments Per Kilobase of transcript per Million mapped reads) RNA expression values for *TBX21* and *ZEB2*. Middle: representative (n = 4) histogram depiction of T-bet expression by flow cytometry; Bottom: T-bet MFI (n = 4, Mean ± SD).

(legend continued on next page)

TLR7 and IL-21 Cooperate with IFN-γ to Induce Human Naive B Cells Differentiation into DN2 and PC

The generation of aNAV and DN2 cells from rNAV B cells was tested under conditions that provide the three categories of signals required for productive B cell activation and differentiation. As combined signal 3 mediators, we selected those inducing hyper-responsiveness of DN2 cells, namely TLR7 and IL-21. Moreover, we included IFN-γ given the prominent expression of T-bet and the role of this cytokine in murine TLR7-induced ABCs (Naradikian et al., 2016). The importance of BCR engagement (signal 1), was tested at different time points as it might be required to trigger naive B cells but might not be necessary for previously activated DN2 cells. We also assessed the role of CD40L (signal 2), as this co-stimulatory signal can inhibit PC differentiation in mice (Randall et al., 1998) and humans (Arpin et al., 1995) and DN2 cells did not respond to CD40L-mediated stimulation (Figure 6A).

In the presence of IFN-γ and IL-21, TLR7 stimulation of SLE and HCD NAV cells generated PC and non-PC progeny including both aNAV and DN2 cells (Figures 7A–7D). Similar cultures showed direct differentiation of aNAV cells into DN2 cells at day 3 and of PC by day 5 (Figure 7E). rNAV from SLE and HCD showed an equivalent ability to generate aNAV and DN2 cells and equivalent PC/non-PC ratios at day 7 indicating an unequivocal stimulation pathway (Figures 7C and 7D). Activation and/or survival was TLR7 dependent as specific inhibition of TLR7 with ODN 20959 (data not shown) or lack of R848 resulted in almost no viable cells by day 7 (< 5% viability, n = 3; Figure 7F). Similar to mouse ABC (Naradikian et al., 2016), the substitution of IFN-γ by IL-4 inhibited the generation of aNAV, DN2 cells, and PC (Figure 7A). Robust PC differentiation also required IL-21, a naive B cell requirement (Figure 7B), and this process was inhibited by continuous BCR signaling or CD40L stimulation (data not shown). CD40L stimulation also inhibited differentiation of rNAV into aNAV and DN2 cells but did not impact the generation of DN1 cells. Combined with the transcriptional similarity between DN1 cells and SWM (Figure 4A), these results strongly suggest that rather than representing DN2 cell precursors, DN1 cells and DN2 B cells belong in separate differentiation pathways. Finally, based on the molecular data suggesting that DN2 cells are poised to undergo PC differentiation, we determined whether this process could be induced by signals 3 alone. Indeed, as shown in Figure 7F, DN2 cell stimulation through TLR7, IL-21, and IFN-γ induced robust PC differentiation in the presence or absence of BCR stimulation. Importantly, PC differentiation required TLR7 as the elimination of R848 resulted in both large increases in cell death and much lower frequencies of PC (Figure 7F). Of note, once normalized for cell number, antibody secretion was equivalent in DN2 cells and SWM cultures with R848 (Figure 7F). Moreover, PC differentiation was efficiently achieved despite lack of DN2 expansion, indicating that extensive cell division is not required for this process (data not shown). Given that PC differentiation is linked to cell division (Nutt et al., 2015), our results further support the notion that a PC differentiation program is already engaged in DN2 cells. Stimulation through combined signals 3 was also sufficient to induce differentiation of autoreactive DN2 cells into PC as indicated by production of anti-Ro, anti-RNP, and anti-Smith antibodies at titers comparable to SWM cells (Figure 7G).

DISCUSSION

We had shown that a large fraction of the ASCs expanded in active SLE derive from a distinct population of aNAV cells and produce disease autoantibodies even in the absence of somatic hypermutation (Tipton et al., 2015). We had also described the expansion in SLE of DN B cells expressing switched, mutated antibodies (Wei et al., 2007). The current study shows that the expansion of DN cells in active SLE is accounted for by distinct DN2 cells that are developmentally related to aNAV cells. DN2 cells are characterized by high expression of CD11c and T-bet; display extra-follicular features, including the absence of CXCR5 and CD62L; and are poised to differentiate into PC. This population is markedly dysregulated and often becomes the predominant B cell population in active SLE, is greatly over-represented in patients with active nephritis, and produces lupus autoantibodies.

Our work identifies the components of the human extra-follicular B cell differentiation pathway through the integration of phenotypic, transcriptional, functional, and repertoire analyses. This approach identifies a developmental link between aNAV and DN2 cells and demonstrates the contribution of this pathway to circulating lupus PB. Moreover, it clarifies the magnitude and the mechanistic basis of enhanced extra-follicular responses in active SLE. The importance of extra-follicular reactions had been well established in mouse models of autoimmunity (Russell et al., 2015; William et al., 2002) but remained unexplored in humans owing to lack of phenotypic identifiers. Further supporting a pathogenic role in human SLE, DN2 cells share the T-bet^{+} CD11c^{bright} phenotype of mouse ABCs, which drive lupus-like autoimmunity in a TLR7-mediated fashion and localize to the T-B cell border (Rubtsova et al., 2017). While an early study failed to document ABC expansion in SLE (Rubtsov et al., 2011), SLE is the autoimmune condition with highest frequency of DN2 cells in an age-independent fashion, a pattern also found in a recent study of CD27^{low}, CD11c^{+} ABC-like B cells (Wang et al., 2018). CD27^{+} T-bet^{+} cells licensed to become PC have also been identified in recall responses as the CD21- activated progeny of memory cells (Lau et al., 2017). Both populations were postulated to represent reactivated post-germinal center memory cells. Thus, our analysis provides needed discrimination of distinct populations with an overlapping T-bet^{+}, CD11c^{hi}, CD21^{lo} phenotype and establishes DN2 cells and aNAV as the main depository of CD11c^{hi} T-bet^{hi} human B cells. Unlike HIV exhausted memory cells, DN2 cells lack FcRL4. Similar to malaria atypical memory cells, DN2 cells express the inhibitory FCRL5,

(E) FPMK values of *TRAF5* and *ZEB1* showing uniquely low expression in DN2 cells (top). Conversely, *TCF7* is expressed only by SWM and DN1 while *BACH2* is expressed only by rNAV (bottom).

(F) Network diagram of select genes upregulated (left) or downregulated (right) in DN2 cells. Transcription factors are green octagons, genes are pink ovals. Arrows represent that motifs for that TF are enriched in a gene and arrows pointing to a TF indicate differential expression of that TF.

Please also see Figures S2–S5.

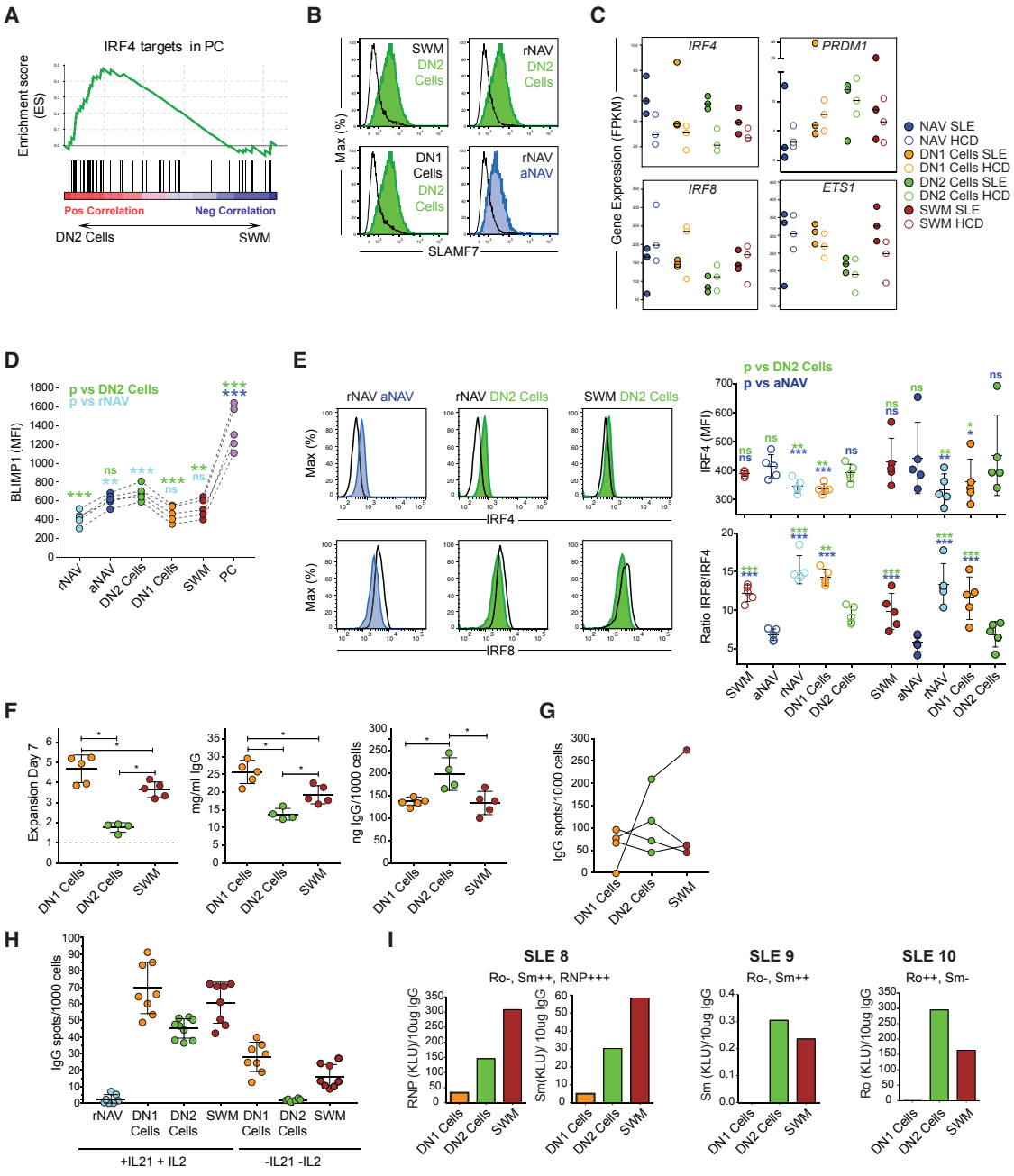

Figure 5. Transcriptional and Functional Characterization of SLE DN2 Cells as Precursors of Autoantibody Producing Plasma Cells

(A) GSEA analysis of RNA-Seq data. DN2 cells are enriched in IRF4 target genes expressed in PC relative to SWM cells.

(B) Flow cytometry histograms demonstrate higher expression in DN2 cells and aNAV cells of SLAMF7, an IRF4 target gene highly expressed by PC.

(C) RNA-Seq analysis shows that DN2 cells express more *IRF4* and *PRDM1* but less *IRF8* and *ETS1* than SWM B cells.

(D) BLIMP1 measurement by flow cytometry. aNAV and DN2 cells have higher expression than other B cells (n = 4, Mean ± SD, repeated-measure one-way ANOVA).

(E) DN2 cells and aNAV cells express more IRF4 than rNAV and DN1 cells and less IRF8 than other B cell subsets and a lower IRF4/IRF8 ratio in both HCD (n = 5) and SLE(n = 5). A representative SLE example is shown on the left and quantification of IRF4 and IRF4/IRF8 ratio is shown on the right (repeated-measure one-way ANOVA).

(F) DN2 cells differentiate into IgG ASC despite little expansion. Replicate wells of day 7 expansion (left), IgG concentration (middle), and IgG concentration normalized to cell number (right). Replicate cultures are shown for 1 out of 4 patients (Mean ± SD, Welch's t test).

(G) The frequency of IgG producing spots does not significantly differ between DN1 cells, DN2 cells, and SWM (n = 4).

(H) Frequency of IgG ASC measured by ELISPOT of B cell subsets stimulated with or without IL-21 and IL-2. Replicate ELISPOT wells are shown for 1 out of 2 patients.

(I) Quantitation of autoantibody production by LIPS assay. DN2 cells cultured as before produce anti-Smith, anti-Ro, and anti-RNP autoantibodies in amounts comparable with SWM cells. Results are shown for three patients as light units normalized to IgG concentration. Serum autoantibody concentrations for the same time point are shown above.

Please also see Figure S6 and S7.

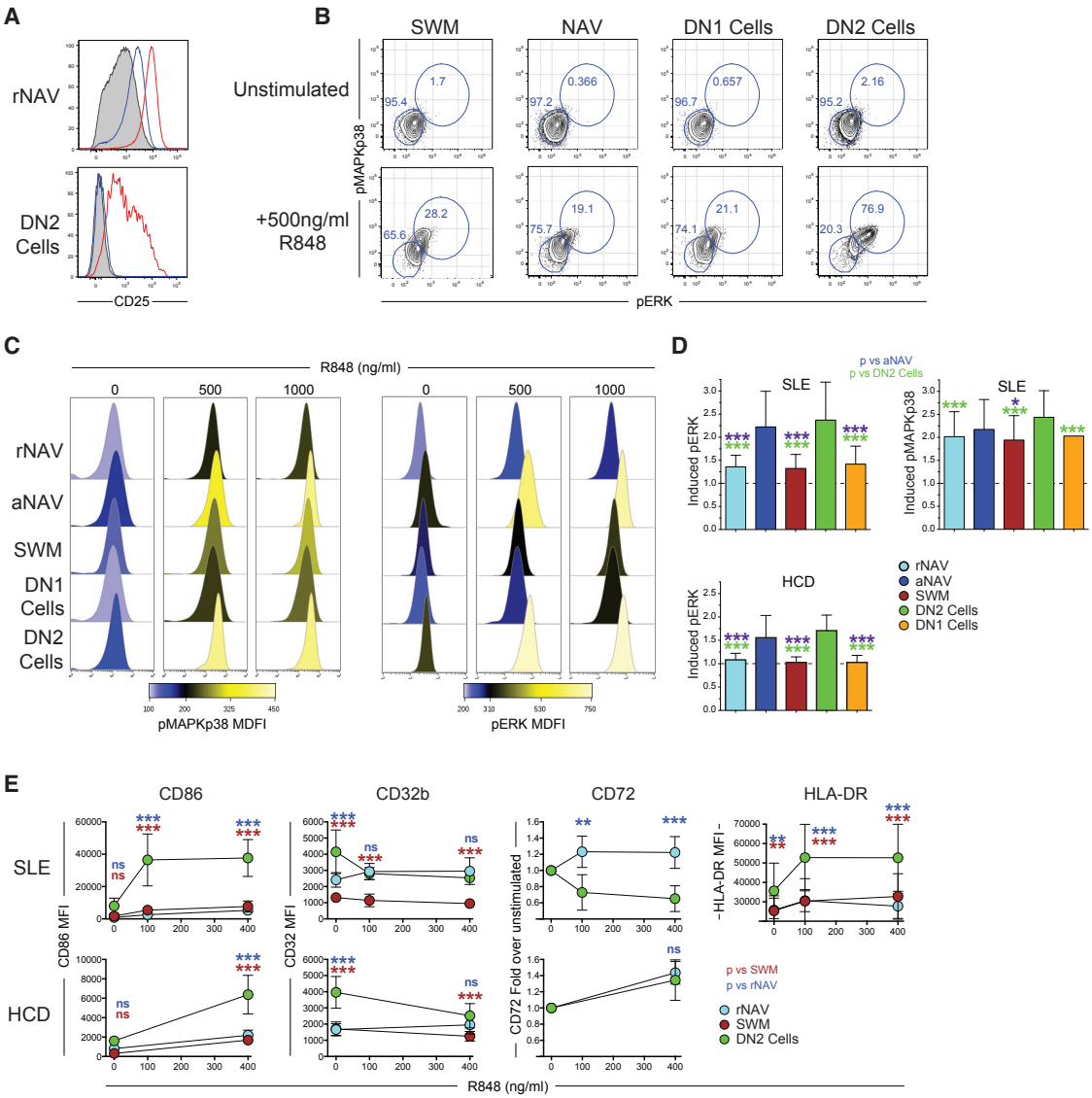

Figure 6. TLR7 Signaling and Responsiveness Is Enhanced in DN2

(A) CD25 expression is increased over baseline (filled) by trimerized CD40L stimulation (blue line) in rNAV but not DN2 cells. In contrast TLR7 stimulation by R848 (red line) increased CD25 expression in both rNAV and DN2 cells. One example out of two experiments is shown.

(B) The percentage of dual positive phospho-ERK and phospho-MAPKp38 positive CD11c$^+$ DN cells is increased after R848 stimulated (bottom) relative to unstimulated (top) and to SWM, rNAV, and DN1 B cells.

(C) Fluorescence intensity of phospho-ERK and phospho-MAPKp38 is higher in DN2 cells and aNAV cells after R848 stimulation. Histogram coloring is based on median fluorescence intensity as shown by the scale bars.

(D) Relative induction of pERK (n = 5) and pMAPKp38 (n = 10), expressed as the fold increase in MFI of R848 stimulated samples, is higher in DN2 cells and aNAV cells. Although induced pY-ERK phosphorylation is lower in HCD B cells (n = 7), DN2 and aNAV cells still have significantly higher phosphorylation (repeated-measure one-way ANOVA).

(E) In SLE patients HLA-DR (n = 6) and CD86 (n = 5) expression is higher at baseline in DN2 cells (green) than NAV (blue) or SWM (red) but this difference is further enhanced after TLR7 stimulation. Expression of inhibitory receptors CD32b and CD72 is reduced by R848 stimulation in DN2 cells (blue) but not NAV B cells (green) (n = 5). HCD B cells demonstrated similar changes except for CD72, which did not decrease in either rNAV or DN2 cells. Red asterisks indicate significant differences from SWM; blue asterisks indicate significant differences from NAV (repeated-measure one-way ANOVA).

yet display conserved BCR signaling. Combined, our results suggest that the expression and/or function of inhibitory receptors is impaired in SLE DN2 cells. This model is strongly supported by the overexpression of other inhibitory receptors such as CD22 despite the overall evidence for activation and propensity for PC differentiation. Of particular significance, DN2 cells are defective in the expression of Ets-1, a CD22-regulated TF that prevents PC differentiation (Luo et al., 2014). Importantly, Ets1 deficiency leads to accumulation of extra-follicular autoreactive B cells (Russell et al., 2015).

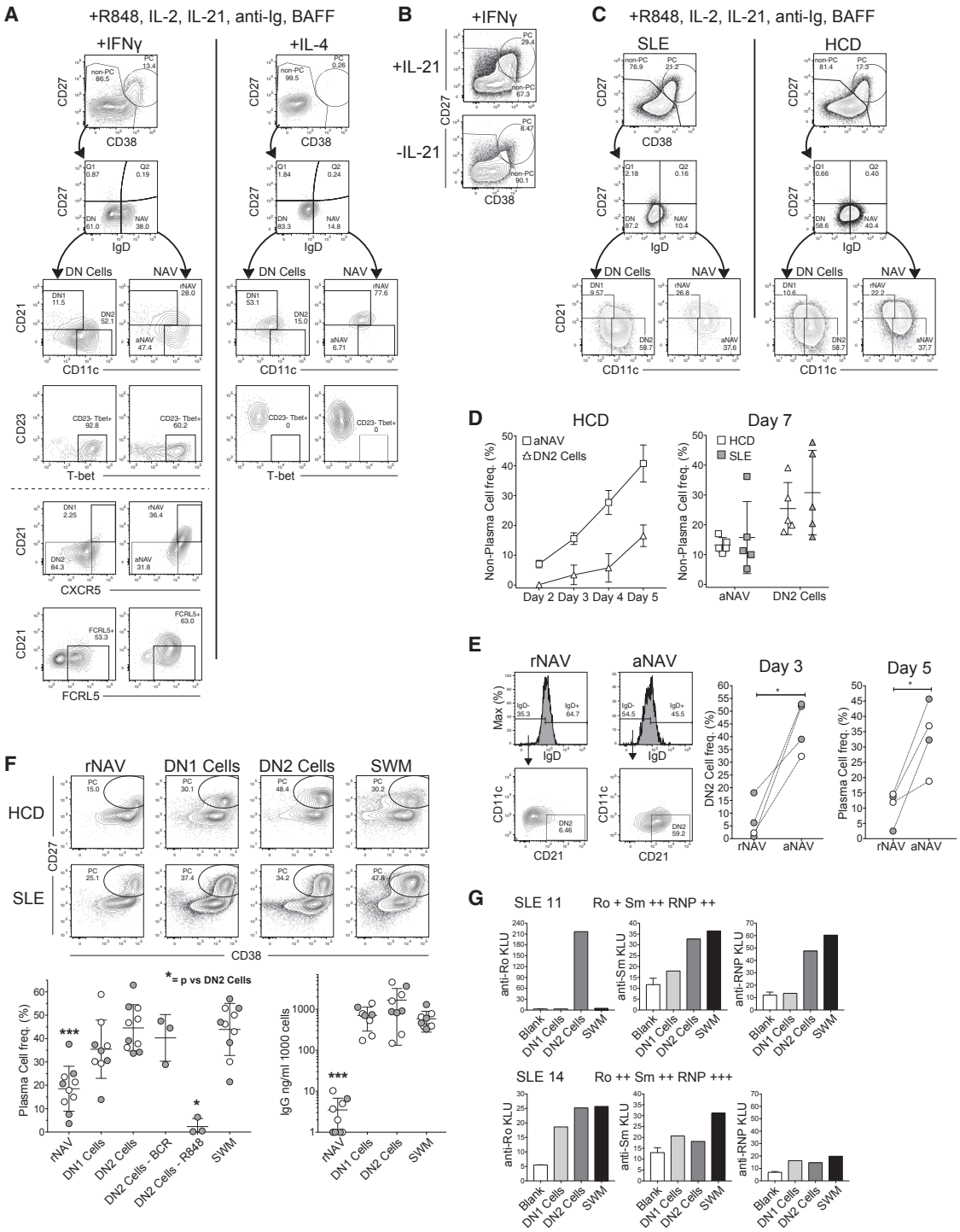

Figure 7. TLR7 and Cytokine Stimulation Induce Differentiation of Naive B Cells into aNAV, DN Cells and PC

(A) TLR7 and IFN-γ (left) but not IL-4 (right) induce aNAV, DN2 cells, and PC differentiation from HCD resting naive (rNAV) B cells in an IL-21 dependent manner. Cells from cultures featuring IFN-γ and IL-21 reproduce the *in vivo* phenotype of aNAV and DN2 cells with CD11c, T-bet, and FCRL5 upregulation (bottom left).

(B) IL-21 is required for day 7 PC development within the IFN-γ cultures from HCD rNAV cells. Similar results were obtained with SLE B cells (not shown).

(C) rNAV cells from both SLE patients and HCD stimulated with TLR7 agonist and cytokines differentiate into PC, DN2 cells, and aNAV B cells with equal efficiency (representative examples; n = 5).

(D) Kinetics of the development of aNAV and DN2 cells from rNAV cultures from HCD (left). Frequencies of aNAV and DN2 cells in the non-PC fraction of day 7 HCD and SLE cultures (right).

(legend continued on next page)

SLE DN2 cells and aNAV cells express an effector transcriptional profile and are poised to differentiate into PC. These properties are illustrated by the absence of BACH2, a TF that inhibits terminal differentiation of PC and $CD8^+$ T cells. DN2 cells and aNAV also express the highest amount of T-bet and T-bet-induced *ZEB2* and lack the T-bet repressor *FOXO1*. T-bet cooperates with Zeb2 to promote effector cell differentiation through inhibition of TCF7, a TF critical for a central memory fate also expressed by human memory cells (Dominguez et al., 2015). Hence, we postulate that T-bet and Zeb2 may play a similar role in DN2 B cells which, in contrast to DN1 cells and SWM, express little TCF7. A shared surface phenotype and transcriptome, as well as a lower frequency of SHM, strongly suggest that DN1 cells represent an early SWM precursor that has not yet acquired CD27 expression.

A PC differentiation pathway for DN2 cells is supported by multiple PC markers including SLAMF7 (Lonial et al., 2015), downregulated sIg, PC differentiation transcriptional programs including silencing of BACH2 (the main negative regulator of *PRDM1* transcription), enhanced *PRDM1* chromatic accessibility, and BLIMP-1 expression. DN2 cells also display a high *IRF4*/*IRF8* ratio in the absence of Ets1, a pattern that promotes differentiation into extra-follicular PB. *In vivo* PC differentiation of DN2 cells derived from aNAV cells is documented by clonal inter-connectivity. In all, DN2 cells represent a poised pre-PC stage of pathogenic relevance through the production of disease-related autoantibodies. Thus, as illustrated by anti-SLAMF7 antibodies, (Lonial et al., 2015), available therapeutic agents could target mature PC, extra-follicular PB and their B cell precursors.

Conclusively establishing a developmental relationship aNAV, DN2 cells and PB can be efficiently generated from naive B cells through TLR7 and IFN-γ stimulation in the presence of IL-21. These conditions also generate DN2 cells and PB from aNAV and PB from DN2 cells. Consistent with a poised PC differentiation stage, DN2 cells readily generated PB through signal 3 stimulation provided by TLR7 and IL-21 without the extensive cell division that is obligatory for PC differentiation of follicular B cells (Nutt et al., 2015) or LPS induced murine B cells (Barwick et al., 2016).

Our studies provide mechanistic insights for SLE. DN2 cells are most prominent in African American patients with severe disease and anti-Sm/RNP antibodies which are genetically linked to susceptibility *IRF5* and *IRF7* haplotypes (Salloum et al., 2010). Enhanced responsiveness to TLR7, an innate receptor of central pathogenic significance (Green and Marshak-Rothstein, 2011), may adversely impact B cell tolerance even at the early transitional stage and facilitate expansion of autoreactive B cells (Giltiay et al., 2013; Kolhatkar et al., 2015). Chronic TLR7 stimulation is sufficient to induce $CD11c^+$ B cells and anti-Sm autoantibodies, whereas B cell-specific TLR7 deficiency decreases $CD11c^+$ B cells and prevents lupus-like disease (Jackson et al., 2014). In keeping with those studies, SLE DN2 cells displayed enhanced TLR7 signaling and TLR7-mediated activation, downregulation of inhibitory receptors (e.g., CD72) and increased expression of co-stimulatory molecules, generation of anti-Sm/RNP autoantibodies, and DN2 cell frequencies correlated with anti-Sm/RNP and anti-RNA serum titers. As immune complexes, these autoantibodies are a major source of exogenous RNA, leading to the stimulation of endosomal TLR7, a process that may be inhibited by CD72 (Akatsu et al., 2016). TLR7 hyper-responsiveness would be enhanced by defective expression of TRAF5 (Buchta and Bishop, 2014). In addition, DN2 cells are defective in other negative regulators of pro-inflammatory responses to TNF and TLR, two major pathogenic pathways in SLE, including *NFKBIA* and *TNFAIP3*, and other regulators of innate sensing pathways including *TRAF5* (TLRs) and *TRAF4* (NOD2). Combined with overexpression of other dsRNA and DNA sensors, our results suggest that SLE DN2 B cells may be dysregulated through exaggerated innate stimulation coupled to defective negative regulation of effector pro-inflammatory pathways.

Notably, DN2 cells and aNAV cells are hyper-responsive to IFN-λ, a poorly understood type III IFN implicated in lupus nephritis (Zickert et al., 2016) that enhances B cell TLR7 expression and responses (de Groen et al., 2015). A predominant role of IFN-λ would be consistent with the weak correlation between serum type I IFN activity and DN2 cell frequency and would identify a therapeutic target not covered by current anti-IFN strategies.

In sum, the present study establishes the prominent participation in SLE of a distinct extrafollicular differentiation pathway that ensues from naive B cells and generates autoreactive PC. Together with our previous work, it demonstrates a prominent role for ongoing activation of naive B cells in the generation of SLE autoantibodies despite long-standing B cell memory of similar autoreactivity. Our work also provides insight into the molecular underpinnings of abnormal DN2 cell responses thereby opening avenues for different therapies, segmentation, monitoring, and outcome measurements in SLE.

STAR★METHODS

Detailed methods are provided in the online version of this paper and include the following:

- KEY RESOURCES TABLE
- CONTACT FOR REAGENT AND RESOURCE SHARING
- EXPERIMENTAL MODEL AND SUBJECT DETAILS

(E) Direct differentiation into DN2 cells starting from rNAV or aNAV in 3 day cultures using similar stimulation as before (left and middle). aNAV cells generated significantly more DN2 cells in either HCD (n = 1) or SLE (n = 3) than rNAV. Day 5 cultures started with aNAV cells (2 HCD and 2 SLE; right) contained significantly higher frequencies of PC (Mann Whitney test).

(F) DN2 cell cultures have an equivalent ability to generate PC as SWM and DN1 cell cultures and are superior to rNAV cultures (HCD = open circles; SLE = shaded circles). Representative examples are shown for HCD and SLE (n = 4). TLR7 stimulation, tested by excluding R848 was essential for DN2 cell to PC differentiation (tested in SLE only; bottom left). When normalized to cell number the IgG output of DN2 cell cultures were equivalent to SWM and DN1 cell cultures and superior to rNAV in both HCD and SLE cells (bottom right; Welch's t test).

(G) LIPS analysis of day 7 culture supernatants from two patients with Ro, SmD, and RNP autoantibody titers.

SUPPLEMENTAL INFORMATION

Supplemental Information includes seven figures and two tables and can be found with this article online at https://doi.org/10.1016/j.immuni.2018.08.015.

ACKNOWLEDGMENTS

We are indebted to our patients and healthy volunteers, clinical coordinators (Debbie Campbell, Jennifer Scantlin, Anna Stephens, and Frances Lee) and members of the Sanz and Lee laboratories for their valuable insights into this project. This work was supported by the CHOA and Emory Pediatrics (Kira Smith, Bridget Neary, and Aaron Rae), and the URMC Flow Cytometry Cores (Tim Bushnell). This work was also supported by National Institutes of Health grants: T32-DK007656 (M.C.W.), AR043737 (M.P.; The Hopkins Lupus Cohort), AR069572 (M.P.; The Hopkins Lupus Cohort), U19-AI110483 Autoimmunity Center of Excellence (I.S., J.M.B.), R37-AI049660 (I.S.), P01-AI125180 (I.S., J.M.B., F.E.L., F.E-H.L), P01-AI1078907 (F.E-H.L.), R01-AI110508 (F.E.L.), R01-AI121252 (F.E-H.L.), and U19-AI109962 (F.E.L., F.E-H.L.).

AUTHOR CONTRIBUTIONS

Conceptualization: S.A.J., K.S.C., I.S., E.Z., F.E-H.L., and F.E.L. ; Methodology: S.A.J., K.S.C., E.Z., R.B., X.W., and Z.S.; Software: C.M.T.; Validation: C.D.S. and E.L.B.; Formal Analysis: C.D.S. and U.M.M.; Investigation: S.A.J., K.S.C., A.V.P., C.D.S., E.B., E.Z., R.B., X.W., and Z.S.; Resources: I.S., F.E.L., J.H.A., S.S.L., and T.B.N.; Writing- Original Draft: S.A.J., K.S.C., and I.S.; Visualization: M.C.W.; Supervision: I.S., G.G., F.E-H.L., J.M.B., F.E.L., and C.W.; Funding Acquisition: I.S., F.E.L., F.E-H.L., and J.M.B.; Writing- Review and Editing: All authors reviewed, edited, and approved the manuscript.

DECLARATION OF INTERESTS

The authors declare no competing interests.

Received: February 27, 2017
Revised: March 13, 2018
Accepted: August 13, 2018
Published: October 9, 2018

REFERENCES

Akatsu, C., Shinagawa, K., Numoto, N., Liu, Z., Ucar, A.K., Aslam, M., Phoon, S., Adachi, T., Furukawa, K., Ito, N., and Tsubata, T. (2016). CD72 negatively regulates B lymphocyte responses to the lupus-related endogenous toll-like receptor 7 ligand Sm/RNP. J. Exp. Med. *213*, 2691–2706.

Arpin, C., Déchanet, J., Van Kooten, C., Merville, P., Grouard, G., Brière, F., Banchereau, J., and Liu, Y.J. (1995). Generation of memory B cells and plasma cells in vitro. Science *268*, 720–722.

Barwick, B.G., Scharer, C.D., Bally, A.P.R., and Boss, J.M. (2016). Plasma cell differentiation is coupled to division-dependent DNA hypomethylation and gene regulation. Nat. Immunol. *17*, 1216–1225.

Barwick, B.G., Scharer, C.D., Martinez, R.J., Price, M.J., Wein, A.N., Haines, R.R., Bally, A.P.R., Kohlmeier, J.E., and Boss, J.M. (2018). B cell activation and plasma cell differentiation are inhibited by de novo DNA methylation. Nat. Commun. *9*, 1900.

Buchta, C.M., and Bishop, G.A. (2014). TRAF5 negatively regulates TLR signaling in B lymphocytes. J. Immunol. *192*, 145–150.

Chiche, L., Jourde-Chiche, N., Whalen, E., Presnell, S., Gersuk, V., Dang, K., Anguiano, E., Quinn, C., Burtey, S., Berland, Y., et al. (2014). Modular transcriptional repertoire analyses of adults with systemic lupus erythematosus reveal distinct type I and type II interferon signatures. Arthritis Rheumatol. *66*, 1583–1595.

Ching, K.H., Burbelo, P.D., Tipton, C., Wei, C., Petri, M., Sanz, I., and Iadarola, M.J. (2012). Two major autoantibody clusters in systemic lupus erythematosus. PLoS ONE *7*, e32001.

Davis, R.S., Wang, Y.-H., Kubagawa, H., and Cooper, M.D. (2001). Identification of a family of Fc receptor homologs with preferential B cell expression. Proc. Natl. Acad. Sci. USA *98*, 9772–9777.

de Groen, R.A., Groothuismink, Z.M., Liu, B.S., and Boonstra, A. (2015). IFN-λ is able to augment TLR-mediated activation and subsequent function of primary human B cells. J. Leukoc. Biol. *98*, 623–630.

Dement-Brown, J., Newton, C.S., Ise, T., Damdinsuren, B., Nagata, S., and Tolnay, M. (2012). Fc receptor-like 5 promotes B cell proliferation and drives the development of cells displaying switched isotypes. J. Leukoc. Biol. *91*, 59–67.

Dominguez, C.X., Amezquita, R.A., Guan, T., Marshall, H.D., Joshi, N.S., Kleinstein, S.H., and Kaech, S.M. (2015). The transcription factors ZEB2 and T-bet cooperate to program cytotoxic T cell terminal differentiation in response to LCMV viral infection. J. Exp. Med. *212*, 2041–2056.

Ehrhardt, G.R., Hijikata, A., Kitamura, H., Ohara, O., Wang, J.-Y., and Cooper, M.D. (2008). Discriminating gene expression profiles of memory B cell subpopulations. J. Exp. Med. *205*, 1807–1817.

Giltiay, N.V., Chappell, C.P., Sun, X., Kolhatkar, N., Teal, T.H., Wiedeman, A.E., Kim, J., Tanaka, L., Buechler, M.B., Hamerman, J.A., et al. (2013). Overexpression of TLR7 promotes cell-intrinsic expansion and autoantibody production by transitional T1 B cells. The Journal of Experimental Medicine 210, 2773–2789.

Green, N.M., and Marshak-Rothstein, A. (2011). Toll-like receptor driven B cell activation in the induction of systemic autoimmunity. Semin. Immunol. *23*, 106–112.

Isnardi, I., Ng, Y.-S., Menard, L., Meyers, G., Saadoun, D., Srdanovic, I., Samuels, J., Berman, J., Buckner, J.H., Cunningham-Rundles, C., and Meffre, E. (2010). Complement receptor 2/CD21- human naive B cells contain mostly autoreactive unresponsive clones. Blood *115*, 5026–5036.

Jackson, S.W., Scharping, N.E., Kolhatkar, N.S., Khim, S., Schwartz, M.A., Li, Q.-Z., Hudkins, K.L., Alpers, C.E., Liggitt, D., and Rawlings, D.J. (2014). Opposing impact of B cell-intrinsic TLR7 and TLR9 signals on autoantibody repertoire and systemic inflammation. J. Immunol. *192*, 4525–4532.

Jacobi, A.M., Odendahl, M., Reiter, K., Bruns, A., Burmester, G.R., Radbruch, A., Valet, G., Lipsky, P.E., and Dörner, T. (2003). Correlation between circulating CD27high plasma cells and disease activity in patients with systemic lupus erythematosus. Arthritis Rheum. *48*, 1332–1342.

Janky, R., Verfaillie, A., Imrichová, H., Van de Sande, B., Standaert, L., Christiaens, V., Hulselmans, G., Herten, K., Naval Sanchez, M., Potier, D., et al. (2014). iRegulon: from a gene list to a gene regulatory network using large motif and track collections. PLoS Comput. Biol. *10*, e1003731.

Kardava, L., Moir, S., Wang, W., Ho, J., Buckner, C.M., Posada, J.G., O'Shea, M.A., Roby, G., Chen, J., Sohn, H.W., et al. (2011). Attenuation of HIV-associated human B cell exhaustion by siRNA downregulation of inhibitory receptors. J. Clin. Invest. *121*, 2614–2624.

Kawai, T., and Akira, S. (2010). The role of pattern-recognition receptors in innate immunity: update on Toll-like receptors. Nat. Immunol. *11*, 373–384.

Kolhatkar, N.S., Brahmandam, A., Thouvenel, C.D., Becker-Herman, S., Jacobs, H.M., Schwartz, M.A., Allenspach, E.J., Khim, S., Panigrahi, A.K., Luning Prak, E.T., et al. (2015). Altered BCR and TLR signals promote enhanced positive selection of autoreactive transitional B cells in Wiskott-Aldrich syndrome. J. Exp. Med. *212*, 1663–1677.

Kometani, K., Nakagawa, R., Shinnakasu, R., Kaji, T., Rybouchkin, A., Moriyama, S., Furukawa, K., Koseki, H., Takemori, T., and Kurosaki, T. (2013). Repression of the transcription factor Bach2 contributes to predisposition of IgG1 memory B cells toward plasma cell differentiation. Immunity *39*, 136–147.

Lau, D., Lan, L.Y.-L., Andrews, S.F., Henry, C., Rojas, K.T., Neu, K.E., Huang, M., Huang, Y., DeKosky, B., Palm, A.E., et al. (2017). Low CD21 expression defines a population of recent germinal center graduates primed for plasma cell differentiation. Sci. Immunol. *2*, eaai8153.

Lonial, S., Dimopoulos, M., Palumbo, A., White, D., Grosicki, S., Spicka, I., Walter-Croneck, A., Moreau, P., Mateos, M.V., Magen, H., et al.; ELOQUENT-2 Investigators (2015). Elotuzumab Therapy for Relapsed or Refractory Multiple Myeloma. N. Engl. J. Med. *373*, 621–631.

Luo, W., Mayeux, J., Gutierrez, T., Russell, L., Getahun, A., Müller, J., Tedder, T., Parnes, J., Rickert, R., Nitschke, L., et al. (2014). A balance between B cell receptor and inhibitory receptor signaling controls plasma cell differentiation by maintaining optimal Ets1 levels. J. Immunol. *193*, 909–920.

Moir, S., Ho, J., Malaspina, A., Wang, W., DiPoto, A.C., O'Shea, M.A., Roby, G., Kottilil, S., Arthos, J., Proschan, M.A., et al. (2008). Evidence for HIV-associated B cell exhaustion in a dysfunctional memory B cell compartment in HIV-infected viremic individuals. J. Exp. Med. *205*, 1797–1805.

Musone, S.L., Taylor, K.E., Lu, T.T., Nititham, J., Ferreira, R.C., Ortmann, W., Shifrin, N., Petri, M.A., Kamboh, M.I., Manzi, S., et al. (2008). Multiple polymorphisms in the TNFAIP3 region are independently associated with systemic lupus erythematosus. Nat. Genet. *40*, 1062–1064.

Naradikian, M.S., Myles, A., Beiting, D.P., Roberts, K.J., Dawson, L., Herati, R.S., Bengsch, B., Linderman, S.L., Stelekati, E., Spolski, R., et al. (2016). Cutting edge: IL-4, IL-21, and IFN-γ interact to govern T-bet and CD11c expression in TLR-activated B cells. J. Immunol. *197*, 1023–1028.

Nutt, S.L., Hodgkin, P.D., Tarlinton, D.M., and Corcoran, L.M. (2015). The generation of antibody-secreting plasma cells. Nat. Rev. Immunol. *15*, 160–171.

Portugal, S., Tipton, C.M., Sohn, H., Kone, Y., Wang, J., Li, S., Skinner, J., Virtaneva, K., Sturdevant, D.E., Porcella, S.F., et al. (2015). Malaria-associated atypical memory B cells exhibit markedly reduced B cell receptor signaling and effector function. eLife *4*, e07218.

Racine, R., Chatterjee, M., and Winslow, G.M. (2008). CD11c expression identifies a population of extrafollicular antigen-specific splenic plasmablasts responsible for CD4 T-independent antibody responses during intracellular bacterial infection. J. Immunol. *181*, 1375–1385.

Randall, T.D., Heath, A.W., Santos-Argumedo, L., Howard, M.C., Weissman, I.L., and Lund, F.E. (1998). Arrest of B lymphocyte terminal differentiation by CD40 signaling: mechanism for lack of antibody-secreting cells in germinal centers. Immunity *8*, 733–742.

Rao, R.R., Li, Q., Gubbels Bupp, M.R., and Shrikant, P.A. (2012). Transcription factor Foxo1 represses T-bet-mediated effector functions and promotes memory CD8(+) T cell differentiation. Immunity *36*, 374–387.

Richardson, C., Chida, A.S., Adlowitz, D., Silver, L., Fox, E., Jenks, S.A., Palmer, E., Wang, Y., Heimburg-Molinaro, J., Li, Q.Z., et al. (2013). Molecular basis of 9G4 B cell autoreactivity in human systemic lupus erythematosus. Journal of immunology *191*, 4926–4939.

Rubtsov, A.V., Rubtsova, K., Fischer, A., Meehan, R.T., Gillis, J.Z., Kappler, J.W., and Marrack, P. (2011). Toll-like receptor 7 (TLR7)-driven accumulation of a novel CD11c^{+} B-cell population is important for the development of autoimmunity. Blood *118*, 1305–1315.

Rubtsova, K., Marrack, P., and Rubtsov, A.V. (2015). TLR7, IFNγ, and T-bet: their roles in the development of ABCs in female-biased autoimmunity. Cell. Immunol. *294*, 80–83.

Rubtsova, K., Rubtsov, A.V., Thurman, J.M., Mennona, J.M., Kappler, J.W., and Marrack, P. (2017). B cells expressing the transcription factor T-bet drive lupus-like autoimmunity. J. Clin. Invest. *127*, 1392–1404.

Russell, L., John, S., Cullen, J., Luo, W., Shlomchik, M.J., and Garrett-Sinha, L.A. (2015). Requirement for Transcription Factor Ets1 in B Cell Tolerance to Self-Antigens. Journal of immunology *195*, 3574–3583.

Salloum, R., Franek, B.S., Kariuki, S.N., Rhee, L., Mikolaitis, R.A., Jolly, M., Utset, T.O., and Niewold, T.B. (2010). Genetic variation at the IRF7/PHRF1 locus is associated with autoantibody profile and serum interferon-α activity in lupus patients. Arthritis Rheum. *62*, 553–561.

Scharer, C.D., Blalock, E.L., Barwick, B.G., Haines, R.R., Wei, C., Sanz, I., and Boss, J.M. (2016a). ATAC-seq on biobanked specimens defines a unique chromatin accessibility structure in naïve SLE B cells. Sci. Rep. *6*, 27030.

Tipton, C.M., Fucile, C.F., Darce, J., Chida, A., Ichikawa, T., Gregoretti, I., Schieferl, S., Hom, J., Jenks, S., Feldman, R.J., et al. (2015). Diversity, cellular origin and autoreactivity of antibody-secreting cell population expansions in acute systemic lupus erythematosus. Nat. Immunol. *16*, 755–765.

Wang, S., Wang, J., Kumar, V., Karnell, J.L., Naiman, B., Gross, P.S., Rahman, S., Zerrouki, K., Hanna, R., Morehouse, C., et al.; Autoimmunity Molecular Medicine Team (2018). IL-21 drives expansion and plasma cell differentiation of autoreactive CD11c^{hi}T-bet^{+} B cells in SLE. Nat. Commun. *9*, 1758.

Weckerle, C.E., Franek, B.S., Kelly, J.A., Kumabe, M., Mikolaitis, R.A., Green, S.L., Utset, T.O., Jolly, M., James, J.A., Harley, J.B., and Niewold, T.B. (2010). Network analysis of associations between serum interferon alpha activity, autoantibodies, and clinical features in systemic lupus erythematosus. Arthritis & Rheumatism *63*, 1044–1053.

Wei, C., Anolik, J., Cappione, A., Zheng, B., Pugh-Bernard, A., Brooks, J., Lee, E.-H., Milner, E.C., and Sanz, I. (2007). A new population of cells lacking expression of CD27 represents a notable component of the B cell memory compartment in systemic lupus erythematosus. J. Immunol. *178*, 6624–6633.

William, J., Euler, C., Christensen, S., and Shlomchik, M.J. (2002). Evolution of autoantibody responses via somatic hypermutation outside of germinal centers. Science *297*, 2066–2070.

Xu, H., Chaudhri, V.K., Wu, Z., Biliouris, K., Dienger-Stambaugh, K., Rochman, Y., and Singh, H. (2015). Regulation of bifurcating B cell trajectories by mutual antagonism between transcription factors IRF4 and IRF8. Nature immunology *16*, 1274–1281.

Yeo, L., Lom, H., Juarez, M., Snow, M., Buckley, C.D., Filer, A., Raza, K., and Scheel-Toellner, D. (2015). Expression of FcRL4 defines a pro-inflammatory, RANKL-producing B cell subset in rheumatoid arthritis. Ann. Rheum. Dis. *74*, 928–935.

Zickert, A., Oke, V., Parodis, I., Svenungsson, E., Sundström, Y., and Gunnarsson, I. (2016). Interferon (IFN)-λ is a potential mediator in lupus nephritis. Lupus Sci. Med. *3*, e000170.

Zuniga, R., Markowitz, G.S., Arkachaisri, T., Imperatore, E.A., D'Agati, V.D., and Salmon, J.E. (2003). Identification of IgG subclasses and C-reactive protein in lupus nephritis: the relationship between the composition of immune deposits and FCgamma receptor type IIA alleles. Arthritis Rheum. *48*, 460–470.

STAR★METHODS

KEY RESOURCES TABLE

REAGENT or RESOURCE	SOURCE	IDENTIFIER
Antibodies		
Anti-BLNK pY84 AX647 Clone J117-1278	BD Bioscience	RRID:AB_647182; Cat#558442
Anti-CD11c PE Clone B-ly6	BD Bioscience	RRID:AB_395793; Cat#555392
Anti-CD138 APC Clone B-B4	Miltenyi Biotech	RRID:AB_244212; Cat#130-081-301
Anti-CD138 PerCP-Cy5.5 Clone MI15	BD Bioscience	RRID:AB_400212; Cat#341087
Anti-CD14 Pacific Orange Clone TUK4	Invitrogen	RRID:AB_10392384; Cat#501121206
Anti-CD19 APC-Cy7 Clone SJ25C1	BD Bioscience	RRID:AB_396873; Cat#557791
Anti-CD20 BV421 Clone H1	BD Bioscience	RRID:AB_2738150; Cat#563346
Anti-CD21 PE-Cy5 Clone B-ly4	BD Bioscience	RRID:AB_394028; Cat#551064
Anti-CD22 FITC Clone HIB22	BD Bioscience	RRID:AB_395818; Cat#555424
Anti-CD24 PE-A610 Clone SN3	Invitrogen	RRID:AB_10373691; Cat#MHCD2404
Anti-CD27 BV605 Clone L128	BD Bioscience	RRID:AB_2744351; Cat#562655
Anti-CD27 BV711 Clone L128	BD Bioscience	RRID:AB_2738042; Cat#563167
Anti-CD27 Qdot605 Clone CLB-27/1	Invitrogen	RRID:AB_2556450; Cat#Q10065
Anti-CD3 Pacific Orange Clone UCHT1	Invitrogen	RRID:AB_2536470; Cat#CD0330TR
Anti-CD3 PerCP-Cy5.5 Clone SP34-2	BD Bioscience	Cat#552852
Anti-CD32B APC Clone 4F5	Gift RK	Clone 4F5
Anti-CD38 PE-Cy7 Clone HIT2	Ebioscience	RRID:AB_1724065; Cat#25-0389-41
Anti-CD62L PE Clone DREG-56	BD Bioscience	RRID:AB_2033966; Cat#560966
Anti-CD72 FITC Clone J4-117	BD Bioscience	RRID:AB_396219; Cat#BDB555918
Anti-CD86 PE Clone 2331(FUN-1)	BD Bioscience	RRID:AB_396013; Cat#555658
Anti-CXCR5 APC Clone 51505	R&D	Cat#FAB190A-025
Anti-ERK1/2 pT202/pY204 AX647 Clone 20A	BD Bioscience	RRID:AB_10895978; Cat#561991
Anti-FCRL4 PE Clone 413D12	Biolegend	RRID:AB_1575103; Cat#340203
Anti-FCRL5 PE Clone 509f6	Biolegend	RRID:AB_2104588; Cat#340304
Anti-HLA-DR BUV395 Clone G46-6	BD Bioscience	Cat#565972
Anti-IgD Biotin Clone IA6-2	BD Bioscience	RRID:AB_396112; Cat#555777
Anti-IgD BUV395 Clone IA6-2	BD Bioscience	Cat#563813
Anti-IgD FITC Clone IA6-2	BD Bioscience	RRID:AB_396113; Cat#555778
Anti-IgG BUV737 Clone G18-145	BD Bioscience	Cat#564861
Anti-IgG3 AX647 Clone HP6050	Southern Biotech	Cat#9210-01
Anti-IRF4 Ax488 Clone IRF4-3E4	Biolegend	RRID:AB_2563266; Cat#646405
Anti-IRF8 PE Clone V3GYWCH	Ebioscience	RRID:AB_2572741; Cat#12-9852-80
Anti-KI67 FITC Clone B56	BD Bioscience	RRID:AB_396302; Cat#556026
Anti-MAPKp38 pT180/pY182 AX488 Clone 36/p38	BD Bioscience	RRID:AB_10896152; Cat#562065
Anti-SLAMF-7 PE Clone 162.1	Biolegend	RRID:AB_2239190; Cat#331806
Anti-STAT1 pY701 AX488 Clone 4A	BD Bioscience	RRID:AB_399855; Cat#612564
Anti-STAT3 pY705 AX647 Clone 4P-STAT3	BD Bioscience	RRID:AB_647144; Cat#557815
Anti-T-bet AX647 Clone 4B10	Biolegend	RRID:AB_1595608; Cat#644801
Anti-VH4.34 PacificBlue Clone 9G4	custom conjugated	Clone 9G4
Anti-IgG3 AX647	Southern Biotech	RRID:AB_620170; Cat#HP6050
Goat anti-human IgM FITC	Southern Biotech	Cat#2020-02
Goat anti-human IgD Biotin	Southern Biotech	Cat#2032-08
Goat anti-human-IgA FITC	Southern Biotech	Cat#2050-02

(*Continued on next page*)

Continued

REAGENT or RESOURCE	SOURCE	IDENTIFIER
Goat Anti-human IgA PE	Southern Biotech	Cat#2050-09
AffiniPure F(ab')$_2$ Fragment Goat Anti-Human IgG, F(ab')$_2$ fragment specific	Jackson ImmunoResearch	RRID:AB_2337639; Cat#109-066- 097
Goat anti-human IgG-alkaline phosphatase, Fc specific	Sigma-Aldrich	RRID:AB_258459; Cat#A9544
ChromPure Human IgG, whole molecule antibody	Jackson ImmunoResearch	RRID:AB_2337043; Cat#009-000-003
Human IgG-Fc Fragment cross-adsorbed Antibody	Bethyl	RRID:AB_10634115; Cat#A80-304A
Human IgG-Fc Fragment cross-adsorbed Antibody Alkaline Phosphatase conjugated	Bethyl	RRID:AB_1063071; Cat# A80-304AP
Chemicals, Peptides, and Recombinant Proteins		
Recombinant human IL-2 (carrier-free)	Biolegend	Cat#589102
Recombinant human IL-21 (Carrier-free)	Biolegend	Cat#571202
Recombinant human IFNy (carrier-free)	Biolegend	Cat#570204
Recombinant human BAFF (carrier-free)	Biolegend	Cat#559602
Recombinant human IL4	R&D	Cat#204-IL
R848 TLR7 agonist	Invivogen	Cat#tlrl-r848-5
ODN 20959 TLR7 inhibitor	Miltenyi	Cat#130-105-814
Critical Commercial Assays		
KPL Bluephos AP ELISA Substrate	KPL	Cat#95059-220
Super Block Blocking Reagent	Thermo Scientific	Cat#37515
MultiScreen-IP sterile filter plates	EMD Millipore	Cat#MSIPN4W
Vector Blue Alkaline Phosphatase Substrate Kit	Vector Laboratories	Cat#SK-5300
HiFi Polymerase	KAPA Biosystems	Cat# KK2601
Agencourt AmpureXP SPRI Beads	Beckman Coulter	Cat# A63881
Renilla Luciferase Assay System	Promega	Cat#E2820
FuGENE6 Transfection Reagent	Promega	Cat#E2691
Ovation RNA-Seq System V2	Nugen	Cat#7102-08
True-Nuclear Transcription Factor Buffer Set	Biolegend	Cat#424401
RNeasy Mini Kit	QIAGEN	Cat# 74104
iScript cDNA Synthesis Kit	Bio-Rad	Cat# 1708891
MiSeq Reagent Kit v2 (300-cycles)	Illumina	Cat# MS-102-2002
Platinum Taq Supermix High Fidelity	Thermo Fisher	Cat# 12532016
Deposited Data		
B cell subset RNA Seq data from HCD and SLE	This paper	GEO GSE92387
Experimental Models: Cell Lines		
WISH epithelial cell line	ATCC	RRID:CVCL_1909 Cat#CCL-25
Oligonucleotides		
VH and constant region primers for repertoire analysis		See Table S3
Recombinant DNA		
Renilla luciferase (Ruc) C-terminal fusion protein vector	M. Iadarola	pREN2
Software and Algorithms		
Prism	GraphPad	V7
FlowJo	TreeStar	V10
Cytobank	Cytobank	V 5.4.0
javaGSEA	Broad Institute	V3.0
TopHat		https://ccb.jhu.edu/software/tophat/index.shtml

(*Continued on next page*)

Continued

REAGENT or RESOURCE	SOURCE	IDENTIFIER
Samtools		http://samtools.sourceforge.net/
HTSeq-0.6.1		https://htseq.readthedocs.io/en/release_0.10.0/
SARTools R package (edgeR analyses)		https://github.com/PF2-pasteur-fr/SARTools
NMF R package (heatmap plotting)	-	https://cran.r-project.org/web/packages/NMF/vignettes/NMF-vignette.pdf

CONTACT FOR REAGENT AND RESOURCE SHARING

Further information and requests for resources and reagents should be directed to and will be fulfilled by the Lead Contact, Ignacio Sanz, M.D. (ignacio.sanz@emory.edu).

EXPERIMENTAL MODEL AND SUBJECT DETAILS

SLE patients met at least 4 revised ACR criteria for SLE. Adult healthy control donors, SLE patients (including 1 female pediatric SLE patient), HIV patients, and autoimmune patients were fully consented under ethical and safe protocols approved by the human subjects Institutional Review Boards of Emory University, the University of Rochester, University of Alabama Birmingham, or Johns Hopkins University. Patient demographic information, including sex and clinical information is listed in Table S1. An additional 22 SLE patients with active nephritis (biopsy confirmed nephritis within 1 month or current proteinuria with past biopsy confirmed nephritis) were also recruited. The RNA Seq experiments described in Figure 4, Figure 5, and Figure S2 were performed on B cells from 3 female SLE patients and 2 female HCD and 1 male HCD. The RNA Seq data shown in Figure S4 are from 8 female SLE patients. Sample sizes can be found referenced within the legends of individual figures for summary experimentation.

METHOD DETAILS

Flow cytometry and cell sorting

Peripheral blood mononuclear cells (PBMC) were isolated using either sodium heparin tubes stored overnight followed by Ficoll gradient isolation (Cohort 1) or sodium heparin CPT Tubes isolated on the same day (Cohort 2). For *in vitro* stimulation of sorted HCD DN2 cells, 500 mL of blood was spun at 2,500*g* for 5 minutes, the plasma layer was removed, and PBMC were isolated from the buffy coat by Ficoll gradient. Following this B cells were enriched by magnetic microparticle purification using the EasySep Human B cell Enrichment Kit Without CD43 Depletion. Enriched B cells (HCD) or total PBMC were then sorted by first gating on $CD19^+$ $CD3^-$ non-PC (not $CD27^{++}$ $CD38^{++}$) and then rNAV:IgD^+ $CD27^-$ $CXCR5^+$ $CD11c^-$, DN1: IgD^- $CD27^-$ $CXCR5^+$ $CD11c^{+\ -}$, DN2: IgD^- $CD27^-$ $CXCR5^-$ $CD11c^{++}$, aNAV: IgD^+ $CD27^-$ $CXCR5^-$ $CD11c^{++}$, and SWM: IgD^- $CD27^+$ $CXCR5^+$ $CD11c^{+\ -}$. Antibodies and fluorochromes utilized are listed in Table S2 and the key resources table. Cells were stained at the manufacturers recommended concentration with 10% normal mouse serum to block Fc receptor and non-specific binding. Anti-mouse beads (Bangs) single stained with each fluorochrome were used for compensation. Intracellular staining was done using True-Nuclear Transcription Factor Buffer Set (Biolegend) for fixation and permeabilization. *Ex vivo* binding of $9G4^+$ antibodies to B cells was quantified by staining with 9G4 Pacific Blue (custom labeled) and comparing the median fluorescence intensity of resting naive and switched memory B cells. Flow cytometry data was analyzed using the FlowJo software (Treestar).

Phosphorylation by flow cytometry

Cell signaling was analyzed after 5 minutes stimulation with 10 μg/ml goat F(ab')2 anti-human IgG (Southern Biotech) for BCR signaling or 15 minutes with 100 ng/ml Interferon Lambda 1 or Interferon Alpha or the indicated doses of IL-10 or IL-21 (R&D) for cytokine receptor signaling or the indicated dose of R848 (Invivogen) for TLR7 signaling. Following stimulation cells were fixed with 1.6% paraformaldehyde for 5 minutes and then permeabilized with 90% ice cold methanol (STAT staining) or 70% ice cold methanol (non-STAT staining) and stored at −20°C until staining with the antibodies listed in Table S2. Because CD21 and CXCR5 staining do not survive methanol permeabilization, DN2 cells and aNAV were gated on $CD11c^{++}$ CD20 bright. Phosphorylation was analyzed using both FlowJo and Cytobank software. Signaling was expressed as the fold increase in median fluorescence intensity over unstimulated controls.

RNA sequencing

Cells were sorted from either HCD or SLE patients into NAV cells: IgD^+ $CD27^-$ IgG^- $CD19^+$, DN1 cells: IgD^- $CD27^-$ IgG^+ $CXCR5^+$ $CD19^+$, DN2 cells: IgD^- $CD27^-$ IgG^+ $CXCR5^-$ $CD19^{2+}$, and SWM cells: IgD^- $CD27^+$ IgG^+ $CXCR5^+$ $CD19^+$. Cells were sorted directly

into lysis buffer and RNA was isolated using RNAeasy micro spin columns (QIAGEN) followed by cDNA amplification using RIBO-SPIA (NuGen). 50 base pair single end sequencing ($20x10^6$ to $5x10^6$ reads/sample) was performed using an Illumina HiSeq 2000 sequencer through the Tufts University Genomics core. An additional 8 SLE patients were sorted for rNAV (IgD^+ $CD27^-$ $CD38^+$ $CD24^+$ MTG^-), aNAV (IgD^+ $CD27^-$ $CD24^-$ $CD38^-$ MTG^+), SWM (IgD^- $CD27^+$), and DN2 cells (IgD^- $CD27^-$ $CXCR5^-$).

RNA Sequencing Analysis

Reads were mapped to the human genome (hg19) with TopHat 2.0.13 using default parameters. The aligned reads were transformed with SAMtools to quantify number of reads at the gene level with HTSeq-0.6.1 using default "union" mode. Raw counts were compiled to identify differentially expressed genes with edgeR within the SARTools R pipeline, using TMM normalization and Benjamini-Hochberg for false discovery rate. Statistical analysis and plotting were performed using the R software v.3.2, and NMF R package was used to draw heatmaps. Transcripts are expressed at reads per kilobase per million (RPKM), genes that showed at least a two-fold difference and a false discovery rate (FDR) of < 0.05 were considered differentially expressed. The RNA sequencing analyis shown in Figure S4 was analyzed as previously described (Barwick et al. 2018) with minor modifications.

Gene Set Enrichment Analysis (GSEA)

GSEA was done using javaGSEA through the Broad Institute. For each comparison, all expressed genes were ranked by t-statistic and preranked analysis was used to look at enrichment in the Broad Institute c2: curated gene sets and c7: immunological signature gene sets, and the 3 sets of interferon regulated genes previously examined in SLE (Chiche et al., 2014). Gene sets with less than 15 or more than 500 genes were excluded. A FDR of 0.05 was used as a cut off for enrichment. Only select enriched pathways are shown.

Transcription factor binding motif analysis

The iRegulon (Janky et al., 2014) application for Cytospace was used for transcription factor binding using the default settings. Based on the principal component analysis, genes with high or low expression in SLE B cells and genes with high or low expression in DN2 cells were used as input gene lists. These genes lists were then analyzed to determine what known and predicted transcription factor binding motifs are enriched, which transcription factors bind these motifs, and which genes in the list have the motif

In vitro stimulation

To test changes in cell surface staining after TLR7 stimulation total B cells were purified from PBMCs by negative selection using magnetic microparticles (StemCell Technologies) and cultured overnight with the indicated doses of R848 in RPMI plus 10% FBS at 37°C in 5% CO2. Because of overnight changes in surface expression, SWM were gated based on IgD- and DN2 cells based on IgD-, CD11c bright, and CD19 bright. To test antibody production, sorted B cells were plated at 20,000-30,000 cells/well in 200 μL RPMI plus 10% FBS stimulated with 1.25 μg/ml R848 (Invivogen), 10 μg/ml goat F(ab')2 anti-human IgG (Southern Biotech), and the following recombinant cytokines (R&D); 50 ng/ml IL-2, 100 ng/ml IL-21, 250 ng/ml IL-10, and 100 ng/ml BAFF.

Stimulation of B cells under Th1 conditions used the following TLR (Invivogen) and cytokine stimuli (Biolegend) in RPMI+10% FBS supplemented with non-essential amino acids, glutamine, sodium pyruvate, and Primocin (Invivogen); R848 1 μg/ml, BAFF 10 ng/ml, IL-21 10ng/ml, IL-2 50 units/ml and IFN-γ 20ng/ml, with or without 10 μg/ml goat F(ab')2 anti-human IgG and IgM for 3 days, cells were then washed and resuspended in fresh media with R848 and cytokines but not anti-IgG and IgM. After 4 additional days (Day 7) cells were counted and, in some experiments plated for ELISPOT, and in others stained for flow cytometry with CD19, IgD, CD27, CD11c, CD21, and CD38 to determine plasma cell differentiation. Cultures may have been initiated with different starting sorted B cell populations and could lack BCR or TLR depending on the questions trying to be addressed. These data representing these cultures will be clearly labeled within their respective figure legends. Supernatants were tested by total IgG ELISA and LIPS assay for autoantigens.

Anti-RNA ELISA

Modified from a protocol generously provided by the laboratory of Mark Shlomchik. Nunc Polysorp flat-bottom plates (Thermo Scientific) were coated overnight at 4°C with poly-L-lysine (Sigma), followed by a 1 hr incubation with 15 μg/mL yeast RNA (Sigma) followed by blocking for 1 hour with PBS+1%BSA. Plates were then washed again, followed by an incubation with 1:10 diluted patient serum samples for 1 hr at room temperature and then washed. Goat anti-human (Fc specific) IgG-AP (Sigma) secondary antibody was then added for 1 hour at room temperature. After washing the KPL BluePhos Microwell Phosphatase Substrate system was utilized according to manufacturer's specifications (Sera Care).

IgG ELISA

Costar Assay plate high binding plates were coated overnight at 4°C with 2 ug/ml Goat Anti-Human IgG, $F(ab')_2$ fragment specific in PBS and then washed with PBS 0.1% Tween-20 and blocked with Super Block Blocking Reagent for 45 minutes. Plates were next incubated with culture supernatants and human IgG whole molecule standard for 60 minutes. Bound antibodies were then detected with 1:15,000 secondary Fc specific goat anti-human IgG-alkaline phosphatase (Sigma) followed by chromogenic detection with KPL BluePhos Microwell Phosphatase Substrate.

IgG ELISPOT

MultiScreen-IP sterile filter plates (EMD Millipore) were first wetted with 15 μL 35% ethanol and immediately washed 3 times with sterile H20 and then coated with 5 μg/ml goat anti-human IgG (Bethyl) in PBS overnight at 4°C. Plates were then washed and blocked with RPMI+10% FBS at 37°C for 60 minutes and serially diluted B cells were incubated in RPMI+10% FBS 12-16 hours. After washing IgG was then detected with 1 μg/ml goat anti-human IgG-alkaline phosphatase (Bethyl) and spots were visualized using Vector Blue Alkaline Phosphatase Substrate and quantified using an automated CTL ELISPOT reader.

Interferon Alpha assay activity

Epithelial derived WISH cells were used as an Interferon Alpha reporter cell line and incubated at $5x10^5$ cells/ml with 50% patient serum in Minimal Essential Medium supplemented with 10% FBS, 10 mM HEPES, 2 mM L-glutamine and penicillin-streptomycin for 6 hours at 37°C. After 6 hours, cells were lysed, RNA isolated and cDNA made from total cellular mRNA and Interferon Alpha induced transcripts *MX1*, *PKR*, and *IFIT1* were quantified by reverse transcriptase-PCR. Relative expression was normalized and presented as an INF-α activity score.

Transcription factor binding motif analysis

The iRegulon (Janky et al., 2014) application for Cytospace was used for transcription factor binding using the default settings. Based on the principal component analysis, genes with high or low expression in SLE B cells and genes with high or low expression in DN2 cells were used as input gene lists. These genes lists were then analyzed to determine what known and predicted transcription factor binding motifs are enriched, which transcription factors bind these motifs, and which genes in the list have the motif. Only the top binding transcription factors with significant enrichment are reported.

Luciferase Immunoprecipitation Systems (LIPS)

LIPS was performed in a 96-well plate format by incubating cell culture supernatant with Renilla luciferase (Ruc)-antigen fusion protiens to the SLE auto-antigens Smith-D, Ro-60, and RNP-U1 (gift of M. Iadarola) for 30 minutes. The antibody-antigen mixture was then captured by proteinA and G beads in a 96-well filter plate. After washing, antibody bound Ruc-antigen is measured using coelenterazine substrate and light units were measured in a Berthold LB 960 Centro luminometer.

ATAC-seq preparation and analysis

ATAC-seq was performed on 10,000-50,000 FACS isolated cells as previously described in detail (Scharer et al., 2016a). Briefly, sorted B cell subsets: rNAV (IgD^+ $CD27^-$ $CD38^+$ $CD24^+$ MTG^-), aNAV (IgD^+ $CD27^-$ $CD24^-$ $CD38^-$ MTG^+), SWM (IgD^- $CD27^+$), and DN2 cells (IgD^- $CD27^-$ $CXCR5^-$) were resuspended in 50 μL Nuclei Lysis Buffer (10 mM Tris-HCl [pH 7.4], 10 mM NaCl, 3 mM MgCl2, 0.1% IGEPAL CA-630) and centrifuged for 30 min at 500xg at 4°C to isolate nuclei. Nuclei were transposed in 25 μL tagmentation reaction buffer (2.5 μL Tn5, 1x Tagment DNA Buffer) and incubated for 1 hr at 37°C. Next, transposed nuclei were lysed with 25 μL 2x Lysis Buffer (300cmM NaCl, 100cmM EDTA, 0.6% SDS, 1.6cμg Proteinase-K) for 30 min at 40°C, low molecular weight DNA purified by size-selection with SPRI-beads (Agencourt), and PCR amplified using Nextera primers with 2x HiFi Polymerase Master Mix (KAPA Biosystems). Amplified, low molecular weight DNA was isolated using a second SPRI-bead size selection. Libraries were sequenced using a 50bp paired-end run at the NYU Genome Technology Center. Raw sequencing reads were mapped to the hg19 version of the human genome using Bowtie and peaks called using MACS2 (Scharer et al., 2016a). Data display and peak quantitation performed using the R/Bioconductor package and custom scripts that are available upon request.

Sample preparation and Illumina MiSEQ sequencing for repertoire analysis

RNA was extracted from lysed samples by following the quick start protocol from QIAGEN's RNeasy Mini Kit. Subsequently, first-strand cDNA synthesis was performed using the iScript cDNA synthesis kit and 8ul of RNA following manufacturer's recommended protocol. First-round amplification of IgG, IgA, and IgM was performed in a 25ul reaction volume using 4ul of cDNA, 20ul Platinum PCR SuperMix High Fidelity (Invitrogen), and 1ul gene specific primers (120nM). PCR1 conditions were as follows: 95°C for 3 minutes; 40 cycles of:30 s 95°C, 30 s 58°C, 30 s 72°C; and 72°C for 5 minutes. Samples were then ligated in a second-round PCR with Nextera Index kit (Illumina). PCR2 conditions for this reaction were as follows: 72°C for 3 minutes; 98°C for 30 s; and 5 cycles of:98°C for 10 s, 63°C for 30 s, and 72°C for 3 minutes. Products was then purified with Agencourt AMPure XP beads (Beckman Coulter). Purified samples were run on 1.2% agarose gels (Lonza) to verify amplification. Libraries were prepared for MiSEQ sequencing by denaturing sample using 0.2N NaOH and quenching the reaction with cold HT1 according to manufacturer's workflow (Illumina). Denatured libraries were combined with 20% PhiX (Illumina) as an internal quality control, then loaded onto a 600-cycle V3 MiSEQ cartridge (Illumina). Emulsion single cell PCR was done on either freshly isolated $CD27^{2+}$ $CD38^{2+}$ plasma cells or DN2 cells stimulated under the conditions described above for 7 days.

B cells were resuspended in PBS (aqueous phase) at a concentration of 100,000/ml and were then passed through the innermost needle of 26-gauge diameter of the flow focusing device at flow rate of 500 μL/min. Then, 45 μL/ml poly(dT) magnetic beads per ml of the cell solution were pelleted using a magnetic strip and fully resuspended in cell lysis buffer (100 mM Tris pH 7.5, 500 mM LiCl, 10 mM EDTA, 1% lithium dodecyl sulfate and 5 mM DTT) and kept on ice. Beads in lysis buffer (aqueous phase) are passed through the 19- gauge outer hypodermic needle at flow rate of 500 μL/min and the oil phase with surfactants (molecular biology grade mineral oil containing 4.5% Span-80, 0.4% Tween 80 and 0.05% Triton X-100, v/v% was passed through the outermost glass tubing with

nozzle (diameter 150 μM) at a flow rate of 3ml/min. The emulsion stream were then serially collected in 2ml centrifuge tubes and kept at room temperature for 2 minutes and then kept on ice for 20 minutes. After 20 minutes, all the tubes were pooled together in 50 mL conical tube and centrifuged at 4000*g* for 5 min at 4°C. Top layer containing oil and smaller emulsions was discarded and the remaining emulsion pellet was broken by adding equal volume of ice cold water saturated diethyl ether. This solution was then centrifuged again at 4000*g* for 6 min at 4°C. Supernatant was carefully aspirated leaving the polydT magnetic beads pellet undisturbed and the pellet was resuspended in 1ml of cold wash buffer 1 (100 mM Tris pH 7.5, 500 mM LiCl and 1 mM EDTA), washed, pelleted again and resuspended in 2ml of cold lysis buffer. Beads were pelleted again, washed and resuspended in 1ml of wash buffer 1, pelleted and resuspended in 500 μL of wash buffer 2 (20 mM Tris pH 7.5, 3mM MgCl and 50 mM KCL). Beads were pelleted and finally resuspended in cold OE RT-PCR mix. The resulting bead mix was emulsified in IKA dispersing tube, plated on 96 well PCR plate, thermocycled RT-PCR. cDNA was extracted and nested PCR was performed as preciously described. The nested PCR products were purified by gel extraction to extract > 850 bp product and sequenced on Illumina platform (2X300 cycles).

QUANTIFICATION AND STATISTICAL ANALYSIS

Flow cytometry analysis

All dot plots or contour plots were plotted in FlowJo v.9 or v.10 software (Treestar) whereas histograms were generated in either FlowJo or Cytobank softwares.

Statistical Analysis

Graphpad Prism version 7 software was used for statistical analysis. Multiple groups from the same patient were compared using repeated-measure one-way ANOVA and the Mann Whitney test or Welch's t test were used to compare unmatched samples. The Holm-Sidak correction was utilized for multiple comparisons and the adjusted P value are indicated as * $p < 0.05$, ** $p < 0.01$, *** $p < 0.001$. Fischer's exact test was used for contingency tests and Spearman's Rank-Order correlation for correlation. All error bars show the mean ± standard deviation

DATA AND SOFTWARE AVAILABILITY

RNA-Seq

Raw sequences and normalized gene expression data are currently available at the Gene Expression Omnibus, with the accession number for the data listed as: GSE92387

Ig-Seq

IgSeq software for repertoire analysis is available upon request.